Supporting Information

Heptacyclic Spiro-TADF Emitters with Efficient Long-Wavelength Emission *via* Through-Space Interactions

Sheng-Yi Yang[1#], Zi-Qi Feng[2#], Cheng Liu[1#], Jianyu Zhang[1], Zihao Deng[1], Kai Zhang[3], Fan-Cheng Kong[5], Philip C. Y. Chow[5], Ryan T. K. Kwok[1], Zuo-Quan Jiang[2*], Jacky W. Y. Lam[1*], Liang-Sheng Liao[2, 3*] and Ben Zhong Tang[1, 4*]

[1]Department of Chemistry, Hong Kong Branch of Chinese National Engineering Research Center for Tissue Restoration and Reconstruction, The Hong Kong University of Science and Technology, Clear Water Bay, Kowloon, Hong Kong SAR 999077, China.
[2]Institute of Functional Nano & Soft Materials (FUNSOM), Jiangsu Key Laboratory for Carbon-Based Functional Materials & Devices, Soochow University, Suzhou, Jiangsu 215123, China.
[3]Macao Institute of Materials Science and Engineering, Macau University of Science and Technology, Macau 999078, China.
[4]School of Science and Engineering, Shenzhen Institute of Aggregate Science and Technology, The Chinese University of Hong Kong, Shenzhen (CUHK-Shenzhen), Guangdong 518172, China.
[5]Department of Mechanical Engineering, The University of Hong Kong, Pokfulam, Hong Kong SAR, 999077, China.
*E-mail: zqjiang@suda.edu.cn; chjacky@ust.hk; lsliao@suda.edu.cn; tangbenz@cuhk.edu.cn.
[#]These authors contributed equally to this work.

Contents

1 Experimental Section

1.1 Materials and instruments

All chemicals and reagents were used as received from commercial sources without further purification. Tetrahydrofuran and toluene used in synthetic routes were purified by sodium treatment. ^{1}H NMR and ^{13}C NMR spectra were recorded on a Bruker 400 spectrometer at room temperature. Mass spectroscopy was performed using a Thermo Fisher ISQ Single Quadrupole High-resolution mass spectra (HRMS) were estimated to be a GCT premier CAB048 mass spectrometer. Ultraviolet-visible absorption spectra were measured by a Shimadzu UV-2600 spectrophotometer. Fluorescent and phosphorescent spectra were measured by a Hitachi F-4600 spectrophotometer and FLS980. Thermogravimetric analysis (TGA) was performed by a METTLER TOLEDO TGA1 under nitrogen atmosphere. The temperature increased to 700 ^{o}C with a heating rate of 10 ^{o}C/min. Differential scanning calorimetry (DSC) measurements were performed by a METTLER TOLEDO DSC1 under nitrogen atmosphere. The temperature was increased and decreased with a heating or cooling rate of 10 ^{o}C/min. Molecular geometries were extracted in single crystals and performed by Gaussian 09W program package with density functional theory (DFT) with Beck's three-parameter hybrid exchange functional[1,2] and Lee, and Yang and Parr correlation functional[3] (B3LYP) with 6-31G(d) basic set. Time-dependent density-functional theory (TD-DFT) based on PBE0 functional with the def2-TZVP basis set. Non-covalent interactions (NCI) of intramolecular interactions analyses were carried out by Multiwfn[4] with reduced density gradient (RDG)[5]. The NCI results were plotted via VMD software (version 1.9.3)[6]. Cyclic voltammetry(CV) was performed on a CHI 600D electrochemical work station with a scan rate of 100 mV S^{-1} at room temperature under an argon flow, in which a Pt disk, a Pt plate and a Ag/AgCl electrode were used as working electrode, counter electrode and reference electrode in tetra-n-butylammonium hexa-fluorophosphates (*n*-Bu_4NPF_6, 0.1 M) dichloromethane/ *N*,*N*-dimethylformamide solution, respectively. For calibration, the redox potential of ferrocene/ferrocenium(Fc/Fc^{+}) was measured under the same conditions. The PLQY was measured using Hamamatsu C9920-02G in nitrogen or air atmosphere. Transient spectra were obtained by using Quantaurus-Tau fluorescence lifetime measurement system (C11367-03, Hamamatsu Photonics Co.) in nitrogen atmosphere.

1.2 Single crystal information

A suitable crystal was selected and on a 'Bruker D8 VENTURE' diffractometer. The crystal was kept at 170.0 K during data collection. Using Olex2, the structure was solved with the XT structure solution program using Intrinsic Phasing and refined with the ShelXL refinement package using Least Squares minimisation. The X-ray crystallographic coordinates for structure reported in this study have been deposited at the Cambridge Crystallographic Data Centre (CCDC), under deposition number intermediate **9** (24351462), **CN** (2238546), **PCz-Sp-2CN** (2238547), **TPA-Sp-2CN** (2223305), **PXZ-Sp-2CN** (2239664). These data can be obtained free of charge from The Cambridge Crystallographic Data Centre “http://www.ccdc.cam.ac.uk/data request/cif”.

1.3 Device fabrication process

OLEDs were fabricated on ITO glass substrates layer (110 nm, 15 Ω/square) under a base pressure of 3 × 10^{-6} Torr. The active area of each device is 0.09 cm^2. Deposition rates and thicknesses of all materials were monitored with oscillating quartz crystals. Doping layers were deposited by utilizing two different sensors to monitor the deposition rates of both host material and dopant material. The deposition rate of host was controlled at 0.2 nm s^{-1}, and the deposition rate of the dopant was adjusted according to the volume ratio doped in the host materials. The electroluminescence (EL) and current density-voltage(*J*-*V*) characteristics of the devices were measured by a constant current source (Keithley 2400 SourceMeter) combined with a photometer (Photo Research SpectraScan PR655).

1.4 Syntheses of materials

The intermediates **4**, **5**, and **6** were afforded by nucleophilic addition and electrophilic cyclization as white solids over 80% yield. Compounds **7**, **8**, and **9** derived from compounds **4**, **5**, and **6**, was oxidized by benzeneseleninic anhydride to give diketone derivative over 20% yield. As shown in **Scheme S1**, the targeted small molecules, **2CN**, **PCz-Sp-2CN**, **TPA-Sp-2CN**, and **PXZ-Sp-2CN**, were afforded by condensation reaction over 90 % yield. The target compounds **2CN**, **PCz-Sp-2CN**, **TPA-Sp-2CN**, and **PXZ-Sp-2CN** were fully characterized by using ^{1}H NMR, ^{13}C NMR spectroscopy, and HRMS.

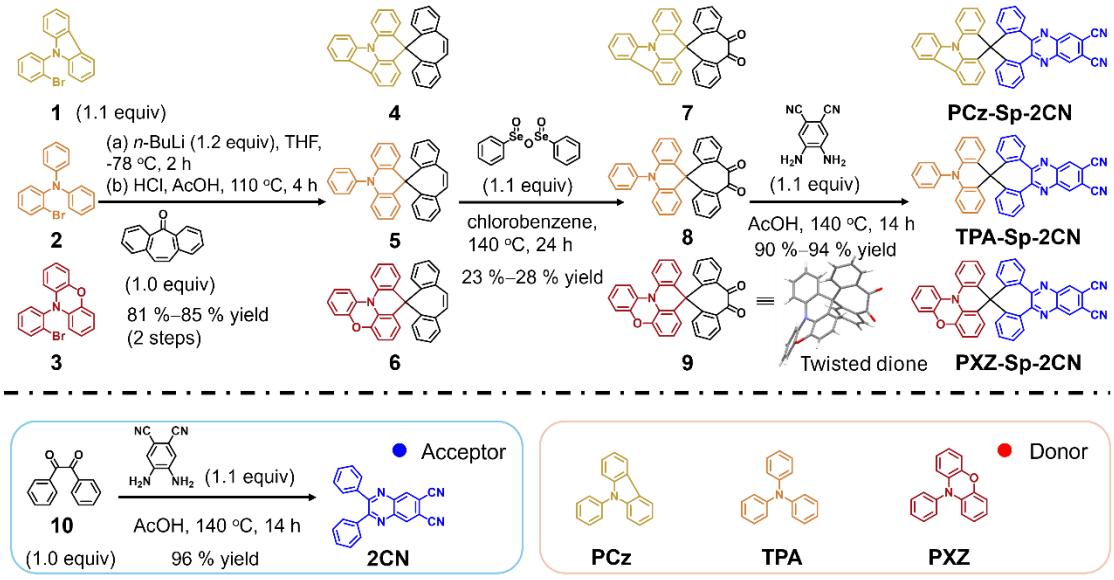

Scheme S1. Synthetic routes to **2CN**, **PCz-Sp-2CN**, **TPA-Sp-2CN**, and **PXZ-Sp-2CN**.

1.4.1 Synthesis of compound **4**

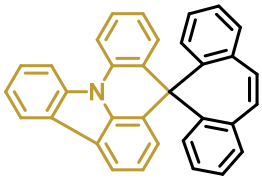

Compound **1**, 9-(2-bromophenyl)-9*H*-carbazole, (1.00 g, 3.12 mmol) was dissolved in 30 mL tetrahydrofuran in a 200 mL Schlenk tube under argon. After the solution was cooled to -78 ^{o}C, *n*-butyl lithium (1.4 mL, 3.42 mmol) was added dropwise via a syringe. The resulting mixture was allowed to stir for 1 hour at -78 ^{o}C, and then 5*H*-dibenzo[a,d][7]annulen-5-one (0.58 g, 2.83 mmol) in 20 mL tetrahydrofuran was added over a period of 10 minutes. After 2 hours reaction at -78 ^{o}C, the mixture was gradually allowed to warm up to room temperature 3 hours. 5 mL water was added to the mixture and tetrahydrofuran was evaporated under reduced pressure. The resulting solid was dissolved in 100 mL dichloromethane and washed with water (3 × 50 mL). Then the organic layer was separated, dried over sodium sulfate, filtered and evaporated, resulting in 1.20 g white solid, which was directly used in the next reaction without further purification. The crude product was dissolved in 30 mL acetic acid and 8 mL hydrochloric acid (36%). After 4 hours reaction at 110 ^{o}C, the reaction was cooled to room temperature, filtered and washed with petroleum ether. The resulting solid was further purified by column chromatography using petroleum ether/ dichloromethane (3/2, v/v) as eluent to afford a white powder (1.14 g, 85%). ^{1}H NMR (400 MHz, Chloroform-*d*) δ 8.31 (dd, *J* = 8.6, 2.1 Hz, 1H), 8.20 (ddd, *J* = 11.2, 8.1, 1.8 Hz, 2H), 7.83 (dq, *J* = 7.7, 1.2 Hz, 1H), 7.64 (ddd, *J* = 8.4, 7.1, 1.3 Hz, 1H), 7.50 – 7.37 (m, 3H), 7.36 – 7.29 (m, 1H), 7.24 – 7.13 (m, 3H), 7.07 – 6.94 (m, 3H), 6.90 – 6.80 (m, 4H), 6.64 – 6.56 (m, 2H). ^{13}C NMR (101 MHz, Chloroform-*d*) δ 147.2, 138.9, 137.7, 135.9, 134.3, 133.4, 133.1, 131.7, 131.6, 130.5, 127.6, 126.7, 126.1, 126.1, 125.6, 123.0, 122.5, 121.2, 120.5, 120.2, 116.8, 113.1, 112.6, 57.0. HRMS (m/z) of $C_{33}H_{21}N$ for [M]: calcd. 431.1674; found, 431.1667.

1.4.2 Synthesis of compound **5**

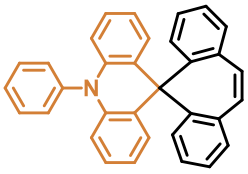

Compound **2**, 2-bromo-*N*,*N*-diphenylaniline, (1.00 g, 3.10 mmol) was dissolved in 30 mL tetrahydrofuran in a 200 mL Schlenk tube under argon. After the solution was cooled to -78 ^{o}C, *n*-butyl lithium (1.4 mL, 3.42 mmol) was added dropwise via a syringe. The resulting mixture was allowed to stir for 1 hour at -78 ^{o}C, and then 5*H*-dibenzo[a,d][7]annulen-5-one (0.58 g, 2.83 mmol) in 20 mL tetrahydrofuran was added over a period of 10 minutes. After 2 hours reaction at -78 ^{o}C, the mixture was gradually allowed to warm up to room temperature 3 hours. 5 mL water was added to the mixture and tetrahydrofuran was evaporated under reduced pressure. The resulting solid was dissolved in 100 mL dichloromethane and washed with water (3 × 50 mL). Then the

organic layer was separated, dried over sodium sulfate, filtered and evaporated, resulting in 1.15 g white solid, which was directly used in the next reaction without further purification. The crude product was dissolved in 30 mL acetic acid and 8 mL hydrochloric acid (36%). After 4 hours reaction at 110 ^{o}C, the reaction was cooled to room temperature, filtered and washed with petroleum ether. The resulting solid was further purified by column chromatography using petroleum ether/ dichloromethane (3/2, v/v) as eluent to afford a white powder (1.08 g, 81%). ^{1}H NMR (400 MHz, Chloroform-*d*) δ 7.69 (t, *J* = 7.7 Hz, 2H), 7.59 – 7.53 (m, 1H), 7.47 – 7.40 (m, 2H), 7.25 – 7.13 (m, 6H), 7.01 (dd, *J* = 6.0, 3.4 Hz, 4H), 6.81 (ddd, *J* = 8.6, 7.1, 1.6 Hz, 2H), 6.64 (ddd, *J* = 8.1, 7.1, 1.3 Hz, 2H), 6.52 (s, 2H), 6.20 (dd, *J* = 8.4, 1.3 Hz, 2H). ^{13}C NMR (101 MHz, Chloroform-*d*) δ 148.9, , 140.5, 136.7, 136.2, 134.1, 132.7, 131.3, 131.0, 130.8, 130.5, 130.2, 127.8, 127.5, 125.8, 125.1, 120.2, 113.3, 56.6. HRMS (m/z) of $C_{33}H_{23}N$ for [M]: calcd. 433.1830; found, 433.1808.

1.4.3 Synthesis of compound **6**

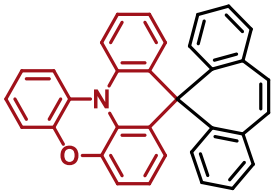

Compound **3**, 10-(2-bromophenyl)-10*H*-phenoxazine, (1.00 g, 2.97 mmol) was dissolved in 30 mL tetrahydrofuran in a 200 mL Schlenk tube under argon. After the solution was cooled to -78 ^{o}C, *n*-butyl lithium (1.3 mL, 3.27 mmol) was added dropwise via a syringe. The resulting mixture was allowed to stir for 1 hour at -78 ^{o}C, and then 5*H*-dibenzo[a,d][7]annulen-5-one (0.56 g, 2.70 mmol) in 20 mL tetrahydrofuran was added over a period of 10 minutes. After 2 hours reaction at -78 ^{o}C, the mixture was gradually allowed to warm up to room temperature 3 hours. 5 mL water was added to the mixture and tetrahydrofuran was evaporated under reduced pressure. The resulting solid was dissolved in 100 mL dichloromethane and washed with water (3 × 50 mL). Then the organic layer was separated, dried over sodium sulfate, filtered and evaporated, resulting in 1.19 g white solid, which was directly used in the next reaction without further purification. The crude product was dissolved in 30 mL acetic acid and 8 mL hydrochloric acid (36%). After 4 hours reaction at 110 ^{o}C, the reaction was cooled to room temperature, filtered and washed with petroleum ether. The resulting solid was further purified by column chromatography using petroleum ether/ dichloromethane (3/2, v/v) as eluent to afford a white powder (1.09 g, 82%). ^{1}H NMR (400 MHz, Chloroform-*d*) δ 7.59 (dd, *J* = 8.4, 1.2 Hz, 1H), 7.53 – 7.47 (m, 1H), 7.22 (dd, *J* = 7.9, 1.5 Hz, 1H), 7.19 – 7.13 (m, 2H), 7.10 (ddd, *J* = 8.5, 7.1, 1.6 Hz, 1H), 7.07 – 6.89 (m, 9H), 6.85 (ddd, *J* = 8.3, 7.2, 1.3 Hz, 1H), 6.81 (dd, *J* = 5.7, 3.7 Hz, 1H), 6.75 – 6.69 (m, 2H), 6.53 (s, 2H). ^{13}C NMR (101 MHz, Chloroform-*d*) δ 148.8, 145.8, 138.5, 136.1, 133.8, 132.2, 131.8, 131.1, 127.0, 126.5, 126.2, 126.2, 123.6, 123.5, 123.2, 117.5, 116.3, 115.6, 113.6, 57.0. HRMS (m/z) of $C_{33}H_{21}NO$ for [M]: calcd. 447.1623; found, 447.1617.

1.4.4 Synthesis of compound **7**

In a two-neck flask, compound **4** (1.00 g, 2.32 mmol), benzeneseleninic anhydride (0.92 g, 2.55 mmol) were dissolved in 20 mL chlorobenzene under nitrogen atmosphere. The mixture was stirred and heated at 140 °C for 24 hours. After cooling to room temperature, the mixture was concentrated under reduced pressure to remove chlorobenzene and then extracted by dichloromethane (3 × 20 mL). The resulting solid was further purified by column chromatography using petroleum ether/ dichloromethane (2/2, v/v) as eluent to afford a yellow powder (0.30 g, 28%). ^{1}H NMR (400 MHz, Chloroform-*d*) δ 8.32 – 8.22 (m, 2H), 8.19 (ddd, *J* = 7.7, 1.4, 0.7 Hz, 1H), 7.85 (dd, *J* = 7.7, 1.0 Hz, 1H), 7.82 – 7.77 (m, 2H), 7.65 (ddd, *J* = 8.5, 7.3, 1.4 Hz, 1H), 7.43 (td, *J* = 7.6, 0.8 Hz, 1H), 7.38 – 7.26 (m, 4H), 7.25 – 7.21 (m, 1H), 7.13 (t, *J* = 7.7 Hz, 1H), 7.07 – 7.00 (m, 2H), 6.93 (ddd, *J* = 8.2, 7.1, 1.1 Hz, 1H), 6.84 (dd, *J* = 7.9, 1.6 Hz, 1H), 6.72 (dd, *J* = 7.7, 0.9 Hz, 1H). ^{13}C NMR (101 MHz, Chloroform-*d*) δ 198.6, 148.3, 134.7, 134.1, 133.7, 133.1, 132.8, 130.3, 128.1, 127.5, 126.9, 126.5, 125.5, 125.4, 123.3, 122.6, 122.2, 120.8, 120.7, 117.5, 114.0, 112.8, 59.2. HRMS (m/z) of $C_{33}H_{19}NO_2$ for $[M + Na]^+$: calcd. 484.1313; found, 484.1313.

1.4.5 Synthesis of compound **8**

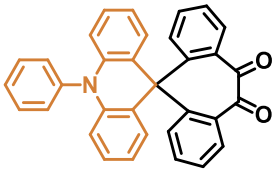

In a two-neck flask, compound **5** (1.00 g, 2.31 mmol), benzeneseleninic anhydride (0.91 g, 2.54 mmol) were dissolved in 20 mL chlorobenzene under nitrogen atmosphere. The mixture was stirred and heated at 140 °C for 24 hours. After cooling to room temperature, the mixture was concentrated under reduced pressure to remove chlorobenzene and then extracted by dichloromethane (3 × 20 mL). The resulting solid was further purified by column chromatography using petroleum ether/ dichloromethane (2/2, v/v) as eluent to afford a yellow powder (0.25 g, 23%). ^{1}H NMR (400 MHz, Chloroform-*d*) δ 7.82 – 7.75 (m, 2H), 7.74 – 7.67 (m, 2H), 7.63 – 7.55 (m, 1H), 7.47 – 7.36 (m, 6H), 7.32 (ddd, *J* = 7.7, 6.7, 1.6 Hz, 2H), 6.87 (ddd, *J* = 8.5, 6.5, 2.2 Hz, 2H), 6.66 – 6.55 (m, 4H), 6.33 – 6.24 (m, 2H). ^{13}C NMR (101 MHz, Chloroform-*d*) δ 199.4, 150.7, 140.5, 138.4, 135.8, 133.6, 131.9, 131.3, 131.1, 130.6, 128.9, 128.8, 128.4, 127.3, 127.1, 121.2, 115.0, 59.8. HRMS (m/z) of $C_{33}H_{21}NO_2$ for [M]: calcd. 463.1572; found, 463.1570.

1.4.6 Synthesis of compound **9**

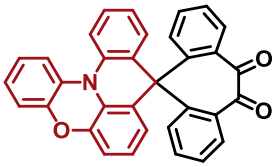

In a two-neck flask, compound **6** (1.00 g, 2.24 mmol), benzeneseleninic anhydride (0.89 g, 2.46 mmol) were dissolved in 20 mL chlorobenzene under nitrogen atmosphere. The mixture was stirred and heated at 140 ^{o}C for 24 hours. After cooling to room temperature, the mixture was concentrated under reduced pressure to remove chlorobenzene and then extracted by dichloromethane (3 × 20 mL). The resulting solid was further purified by column chromatography using petroleum ether/ dichloromethane (2/2, v/v) as eluent to afford a yellow powder (0.27 g, 25%). ^{1}H NMR (400 MHz, Chloroform-*d*) δ 7.63 (dd, *J* = 8.4, 1.2 Hz, 3H), 7.42 – 7.27 (m, 5H), 7.21 – 7.07 (m, 3H), 7.06 – 6.97 (m, 3H), 6.85 (ddd, *J* = 8.2, 7.1, 1.2 Hz, 1H), 6.79 – 6.62 (m, 3H), 6.22 (dd, *J* = 7.8, 1.6 Hz, 1H). ^{13}C NMR (101 MHz, Chloroform-*d*) δ 181.8, 147.9, 145.6, 133.7, 133.4, 131.5, 131.2, 129.9, 126.7, 124.6, 123.6, 123.4, 123.1, 122.8, 117.0, 115.6, 115.4, 113.9, 59.1. HRMS (m/z) of $C_{33}H_{19}NO_3$ for $[M + Na]^+$: calcd. 500.1263; found, 500.1257.

1.4.7 Synthesis of compound **PCz-Sp-2CN**

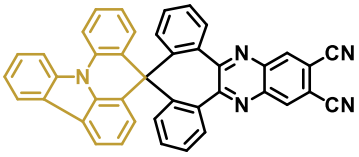

In a two-neck flask, compound **7** (0.50 g, 1.08 mmol), 4,5-diaminophthalonitrile (0.19 g, 1.19 mmol) were dissolved in 20 mL AcOH under nitrogen atmosphere. The mixture was stirred and heated at 120 ^{o}C for 12 hours. After cooling to room temperature, the reaction solution was poured into ice water, and a dark yellow solid was precipitated and suction filtration. Then extracted by dichloromethane (3 × 20 mL). The resulting solid was further purified by column chromatography using petroleum ether/ dichloromethane (1/1, v/v) as eluent to afford a yellow powder (0.59 g, 94%). ^{1}H NMR (400 MHz, Chloroform-*d*) δ 8.65 (s, 2H), 8.24 (dd, *J* = 7.8, 1.6 Hz, 2H), 8.15 (dt, *J* = 7.7, 1.1 Hz, 1H), 8.12 – 8.04 (m, 2H), 7.99 (dd, *J* = 7.6, 1.0 Hz, 1H), 7.56 (ddd, *J* = 8.5, 7.3, 1.4 Hz, 1H), 7.46 – 7.33 (m, 4H), 7.30 (ddd, *J* = 8.7, 7.2, 1.5 Hz, 2H), 7.25 (d, *J* = 7.7 Hz, 1H), 7.19 (ddd, *J* = 8.4, 7.2, 1.5 Hz, 1H), 7.04 (dd, *J* = 8.4, 1.2 Hz, 2H), 6.67 (dd, *J* = 8.1, 1.5 Hz, 1H), 6.52 (ddd, *J* = 8.3, 7.2, 1.2 Hz, 1H). ^{13}C NMR (101 MHz, Chloroform-*d*) δ 156.3, 147.5, 140.9, 137.5, 136.3, 135.3, 132.6, 130.8, 130.0, 129.3, 127.6, 127.1, 126.2, 125.9, 124.5, 122.5, 121.5, 121.5, 121.0, 120.6, 118.4, 114.5, 113.7, 113.5, 56.8. HRMS (m/z) of $C_{41}H_{21}N_5$ for $[M + Na]^+$: calcd. 606.1695; found, 606.1694. Anal. calcd for $C_{41}H_{21}N_5$ (%): C 84.37, H 3.63, N 12.00; found: C 84.42, H 3.59, N 11.99.

1.4.8 Synthesis of compound **TPA-Sp-2CN**

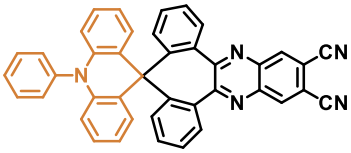

In a two-neck flask, compound **8** (0.50 g, 1.08 mmol), 4,5-diaminophthalonitrile (0.19 g, 1.19 mmol) were dissolved in 20 mL AcOH under nitrogen atmosphere. The mixture was stirred and heated at 120 ^{o}C for 12 hours. After cooling to room temperature, the reaction solution was poured into ice water, and a red solid was precipitated and suction filtration. Then extracted by dichloromethane (3 × 20 mL). The resulting solid was further purified by column chromatography using petroleum ether/ dichloromethane (1/1, v/v) as eluent to afford a pale red powder (0.57 g, 90%). ^{1}H NMR (400 MHz, Chloroform-*d*) δ 8.59 (s, 2H), 8.22 (dd, *J* = 7.6, 1.7 Hz, 2H), 7.59 – 7.52 (m, 2H), 7.51 – 7.39 (m, 5H), 7.28 (dd, *J* = 8.1, 1.4 Hz, 2H), 7.08 – 7.02 (m, 2H), 6.95 – 6.87 (m, 4H), 6.51 (ddd, *J* = 8.0, 7.3, 1.2 Hz, 2H), 6.40 (dd, *J* = 8.3, 1.2 Hz, 2H). ^{13}C NMR (101 MHz, Chloroform-*d*) δ 156.3, 148.3, 141.6, 140.7, 136.2, 135.5, 132.4, 130.8, 130.4, 130.1, 129.7, 129.6, 128.0, 126.9, 126.8, 125.7, 119.0, 114.6, 114.4, 113.2, 55.8. HRMS (m/z) of $C_{41}H_{23}N_5$ for $[M + H]^+$: calcd. 586.2032; found, 586.2024. Anal. calcd for $C_{41}H_{23}N_5$ (%): C 84.08, H 3.96, N 11.96; found: C 84.01, H 4.00, N 11.99.

1.4.9 Synthesis of compound **PXZ-Sp-2CN**

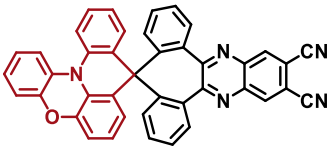

In a two-neck flask, compound **9** (0.50 g, 1.05 mmol), 4,5-diaminophthalonitrile (0.18 g, 1.15 mmol) were dissolved in 20 mL AcOH under nitrogen atmosphere. The mixture was stirred and heated at 120 ^{o}C for 12 hours. After cooling to room temperature, the reaction solution was poured into ice water, and a red solid was precipitated and suction filtration. Then extracted by dichloromethane (3 × 20 mL). The resulting solid was further purified by column chromatography using petroleum ether/ dichloromethane (1/1, v/v) as eluent to afford a deep red powder (0.58 g, 93%). ^{1}H NMR (400 MHz, Chloroform-*d*) δ 8.66 (s, 1H), 8.55 (dd, *J* = 7.5, 2.0 Hz, 1H), 8.49 (s, 1H), 8.39 – 8.31 (m, 1H), 7.70 – 7.55 (m, 3H), 7.52 (dd, *J* = 8.2, 1.2 Hz, 1H), 7.25 – 7.12 (m, 3H), 7.05 (ddd, *J* = 8.4, 7.2, 1.4 Hz, 1H), 6.95 – 6.80 (m, 4H), 6.77 (dd, *J* = 8.1, 1.2 Hz, 1H), 6.72 – 6.62 (m, 2H), 6.59 – 6.49 (m, 2H). ^{13}C NMR (101 MHz, Chloroform-*d*) δ 147.2, 146.3, 144.4, 139.9, 136.2, 136.0, 133.9, 132.5, 132.3, 129.9, 129.6, 129.0, 128.7, 127.8, 127.4, 127.0, 126.6, 124.0, 122.9, 122.7, 121.5, 120.6, 118.0, 116.6, 114.5, 114.0, 113.3, 54.9. HRMS (m/z) of $C_{41}H_{21}N_5O$ for [M]: calcd. 599.1746; found, 599.1749. Anal. calcd for $C_{41}H_{21}N_5O$ (%): C 82.12, H 3.53, N 11.68; found: C 82.18, H 3.57, N 11.63.

1.4.10 Synthesis of reference compound **2CN**

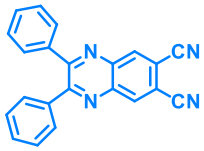

In a two-neck flask, compound **10** (0.42 g, 2.00 mmol), 4,5-diaminophthalonitrile (0.35 g, 2.20 mmol) were dissolved in 20 mL AcOH under nitrogen atmosphere. The mixture was stirred and heated at 120 ^{o}C for 12 hours. After cooling to room temperature, the reaction solution was poured into ice water, and a white solid was precipitated and suction filtration. Then extracted by dichloromethane (3 × 20 mL). The resulting solid was further purified by column chromatography using petroleum ether/ dichloromethane (2/1, v/v) as eluent to afford a white powder (0.63 g, 96%). ^{1}H NMR (400 MHz, Chloroform-*d*) δ 8.63 (s, 2H), 7.60 – 7.52 (m, 4H), 7.50 – 7.43 (m, 2H), 7.43 – 7.31 (m, 4H). ^{13}C NMR (101 MHz, Chloroform-*d*) δ 156.9, 141.0, 136.7, 136.3, 129.8, 129.3, 128.0, 114.4, 113.5. HRMS (m/z) of $C_{22}H_{12}N4$ for $[M + Na]^{+}$: calcd. 355.0960; found, 355.0956.

1.5 Density functional theory

The structural optimization of **2CN**, **PCz-Sp-2CN**, **TPA-Sp-2CN**, and **PXZ-Sp-2CN** were conducted with the geometries obtained from the X-ray crystallographic analyses. The ground state moments of **2CN**, **PCz-Sp-2CN**, **TPA-Sp-2CN**, and **PXZ-Sp-2CN** were obtained using DFT method by adopting B3LYP/6-31g(d) level of theory. TD-DFT calculations were carried out using the PBE0/def2-TZVP functional and basis and the geometries obtained from the X-ray crystallographic analyses.

Cartesian coordinates of **2CN** in ground state:

N	1.45910000	2.44910000	11.03780000
N	2.33510000	3.76190000	13.37970000
N	-2.63000000	2.86440000	16.38200000
N	-4.01840000	1.58200000	12.86920000
C	0.62960000	2.61250000	12.10790000
C	1.09550000	3.19710000	13.30840000
C	0.24570000	3.25440000	14.43690000
H	0.56520000	3.60910000	15.25700000
C	-1.04340000	2.79500000	14.33800000

C	-1.53180000	2.25730000	13.10560000
C	-0.69890000	2.15040000	12.02070000
H	-1.01660000	1.76550000	11.21110000
C	-1.92400000	2.84350000	15.47820000
C	-2.91270000	1.86160000	12.98680000
C	2.68170000	2.92830000	11.13750000
C	3.09570000	3.68550000	12.30570000
C	4.36740000	4.44790000	12.33840000
C	5.21090000	4.33580000	13.43730000
H	4.98470000	3.74840000	14.14720000
C	6.37650000	5.07500000	13.50000000
H	6.95620000	4.98400000	14.24850000
C	6.69960000	5.94410000	12.48020000
H	7.49690000	6.45880000	12.53120000
C	5.85960000	6.06830000	11.37930000
H	6.08280000	6.67080000	10.67760000
C	4.69860000	5.31690000	11.30030000
H	4.13140000	5.39350000	10.54130000
C	3.60690000	2.61280000	10.01830000
C	3.11280000	2.61880000	8.71030000
H	2.20540000	2.84740000	8.54750000
C	3.94440000	2.29240000	7.64880000
H	3.60880000	2.31750000	6.76010000

C	5.26180000	1.93020000	7.87850000
H	5.82720000	1.70270000	7.14950000
C	5.75390000	1.90040000	9.17990000
H	6.65400000	1.63910000	9.33800000
C	4.93640000	2.25050000	10.24530000
H	5.28220000	2.24400000	11.12930000

Cartesian coordinates of **PCz-Sp-2CN** in ground state:

N	7.01030000	8.89890000	2.57810000
N	5.93140000	5.17480000	6.30500000
N	5.31260000	3.11410000	4.49820000
N	8.97850000	1.74480000	9.99530000
N	8.21230000	-1.08250000	7.30940000
C	5.04120000	6.88140000	2.49670000
C	4.92970000	8.07580000	1.53340000
C	3.85430000	8.47720000	0.74350000
H	3.15430000	7.86010000	0.56240000
C	3.78230000	9.77710000	0.20740000
H	3.05150000	10.00520000	-0.35570000
C	4.74640000	10.73170000	0.47720000
H	4.67090000	11.61250000	0.12840000
C	5.82750000	10.37170000	1.27040000
C	5.89420000	9.06030000	1.75320000
C	7.48990000	7.59160000	2.77790000

C	8.85210000	7.31800000	2.96210000
H	9.46990000	8.03000000	3.08170000
C	9.29350000	6.00470000	2.96910000
H	10.20850000	5.81550000	3.14210000
C	8.41590000	4.96890000	2.72710000
H	8.72890000	4.07190000	2.69520000
C	7.07000000	5.24840000	2.52920000
H	6.47760000	4.53450000	2.32290000
C	6.55850000	6.54850000	2.62410000
C	7.68880000	10.13640000	2.60560000
C	8.83800000	10.50280000	3.30440000
H	9.30130000	9.88240000	3.85470000
C	9.27860000	11.81420000	3.16300000
H	10.08000000	12.08170000	3.59790000
C	8.57400000	12.75220000	2.39770000
H	8.89210000	13.64540000	2.33310000
C	7.42060000	12.38480000	1.73780000
H	6.93160000	13.02360000	1.23270000
C	6.97650000	11.06220000	1.82070000
C	4.46190000	7.42310000	3.85700000
C	3.75980000	8.64070000	3.90930000
H	3.56920000	9.09590000	3.09710000
C	3.33780000	9.19660000	5.10100000

H	2.84930000	10.01140000	5.09260000
C	3.61810000	8.57970000	6.30640000
H	3.36680000	8.98300000	7.12910000
C	4.27320000	7.36090000	6.28700000
H	4.46040000	6.92030000	7.10720000
C	4.66670000	6.76380000	5.08010000
C	5.23740000	5.40820000	5.20660000
C	4.91520000	4.35240000	4.27010000
C	4.15230000	4.51660000	2.99980000
C	3.42750000	3.38180000	2.59960000
H	3.32800000	2.65860000	3.20760000
C	2.85520000	3.28990000	1.34500000
H	2.32630000	2.53640000	1.11200000
C	3.06110000	4.30420000	0.43890000
H	2.70680000	4.23520000	-0.43910000
C	3.78970000	5.43460000	0.80820000
H	3.95430000	6.10850000	0.15920000
C	4.28420000	5.60640000	2.10280000
C	6.36700000	3.90580000	6.52310000
C	6.05530000	2.87320000	5.61250000
C	6.52450000	1.56380000	5.84850000
H	6.31300000	0.86600000	5.23890000
C	7.28580000	1.29830000	6.95620000

C	7.57530000	2.33870000	7.90050000
C	7.11910000	3.61950000	7.68250000
H	7.30950000	4.30700000	8.30910000
C	7.80410000	-0.03040000	7.16370000
C	8.36200000	2.02460000	9.07020000

Cartesian coordinates of **TPA-Sp-2CN** in ground state:

N	7.45800000	4.77110000	8.16630000
N	4.37230000	5.76750000	14.46680000
N	6.31680000	7.76300000	14.44530000
N	0.29860000	9.00950000	17.19700000
N	3.21870000	11.64270000	17.54310000
C	8.23150000	3.92390000	8.96370000
C	9.13330000	3.01980000	8.36760000
H	9.26390000	3.03620000	7.42600000
C	9.82820000	2.10920000	9.13890000
H	10.42370000	1.49700000	8.72590000
C	9.66020000	2.08410000	10.52280000
H	10.11510000	1.44050000	11.05170000
C	8.82140000	3.01140000	11.11240000
H	8.72740000	3.01290000	12.05780000
C	8.10750000	3.94690000	10.35590000
C	7.21930000	4.95610000	11.10510000
C	6.50460000	5.89370000	10.11800000

C	5.68580000	6.92030000	10.59540000
H	5.60970000	7.04130000	11.53330000
C	4.98040000	7.76930000	9.75810000
H	4.43660000	8.46150000	10.11470000
C	5.08330000	7.58810000	8.38180000
H	4.59580000	8.14960000	7.78890000
C	5.89470000	6.59250000	7.87900000
H	5.96170000	6.47990000	6.93780000
C	6.62520000	5.74170000	8.72620000
C	7.53650000	4.68670000	6.73360000
C	6.62610000	3.91190000	6.03720000
H	5.98100000	3.39590000	6.50560000
C	6.66170000	3.89390000	4.64530000
H	6.04250000	3.35960000	4.16000000
C	7.60020000	4.65460000	3.96670000
H	7.62190000	4.64780000	3.01860000
C	8.50670000	5.42550000	4.67630000
H	9.14940000	5.94760000	4.20950000
C	8.48370000	5.44130000	6.06390000
H	9.11080000	5.96500000	6.54850000
C	6.15070000	4.08730000	11.82590000
C	5.70410000	2.97220000	11.09160000
H	6.00630000	2.86790000	10.19720000

C	4.84670000	2.02200000	11.61220000
H	4.55600000	1.29400000	11.07470000
C	4.41340000	2.14160000	12.92680000
H	3.89530000	1.45500000	13.33130000
C	4.74940000	3.27520000	13.63310000
H	4.41980000	3.37850000	14.51890000
C	5.56620000	4.29010000	13.08850000
C	5.51700000	5.58420000	13.82180000
C	6.52700000	6.61700000	13.81130000
C	7.85840000	6.52580000	13.15810000
C	8.84040000	7.34020000	13.76050000
H	8.61290000	7.82470000	14.54530000
C	10.11370000	7.46060000	13.25570000
H	10.76250000	7.99580000	13.69740000
C	10.42880000	6.78310000	12.08920000
H	11.29900000	6.85860000	11.71470000
C	9.47390000	5.99670000	11.46930000
H	9.70390000	5.56170000	10.65580000
C	8.17720000	5.81130000	11.98430000
C	4.14930000	6.95430000	15.08930000
C	2.88300000	7.19790000	15.67820000
H	2.20870000	6.52780000	15.66700000
C	2.64470000	8.42010000	16.26700000

C	3.67310000	9.41030000	16.32480000
C	4.89810000	9.19130000	15.73560000
H	5.57350000	9.85840000	15.76260000
C	5.13650000	7.95480000	15.08570000
C	1.33880000	8.72750000	16.80180000
C	3.42000000	10.65690000	17.00170000

Cartesian coordinates of **PXZ-Sp-2CN** in ground state:

O	10.23330000	6.41090000	6.22550000
N	10.27090000	5.23780000	3.71010000
N	5.88300000	3.56560000	5.16850000
N	4.13800000	5.01750000	3.50750000
N	2.91710000	4.49320000	10.13200000
N	0.48800000	6.60540000	7.81530000
C	8.10450000	5.03580000	2.02690000
C	9.49010000	5.29720000	1.40090000
C	9.81200000	5.22630000	0.04710000
H	9.11340000	5.18300000	-0.59530000
C	11.13450000	5.21760000	-0.38280000
H	11.32980000	5.17770000	-1.31180000
C	12.16510000	5.26620000	0.53850000
H	13.06870000	5.26510000	0.24530000
C	11.87280000	5.31580000	1.88940000
H	12.57890000	5.35650000	2.52300000

C	10.54980000	5.30610000	2.32840000
C	9.11380000	5.88400000	4.15500000
C	9.07660000	6.52930000	5.37640000
C	7.99420000	7.31300000	5.72000000
H	7.95120000	7.72600000	6.57410000
C	6.96890000	7.49030000	4.79950000
H	6.24630000	8.07230000	5.00320000
C	6.99410000	6.82100000	3.58230000
H	6.29950000	6.96810000	2.95150000
C	8.02820000	5.93700000	3.27780000
C	11.14950000	5.40170000	5.93060000
C	11.25730000	4.85070000	4.65600000
C	12.14950000	3.81690000	4.44660000
H	12.17080000	3.36680000	3.61150000
C	13.01680000	3.44330000	5.46490000
H	13.66670000	2.76810000	5.30640000
C	12.93940000	4.04410000	6.70500000
H	13.54310000	3.78850000	7.39260000
C	11.98620000	5.02220000	6.95580000
H	11.91130000	5.41980000	7.81560000
C	7.23170000	2.95070000	3.30610000
C	7.30280000	1.59920000	3.65800000
H	6.68470000	1.24840000	4.28810000

C	8.25910000	0.76360000	3.10430000
H	8.30110000	-0.15410000	3.34420000
C	9.15300000	1.30170000	2.19160000
H	9.80530000	0.74190000	1.78720000
C	9.10490000	2.64790000	1.86270000
H	9.74150000	2.99400000	1.24700000
C	8.14730000	3.51550000	2.40900000
C	6.85060000	5.28420000	1.16560000
C	6.90280000	6.01960000	-0.01500000
H	7.72870000	6.40440000	-0.28110000
C	5.78270000	6.20780000	-0.81860000
H	5.85850000	6.69400000	-1.63150000
C	4.55870000	5.68860000	-0.43780000
H	3.80540000	5.75460000	-1.01280000
C	4.44930000	5.07160000	0.79560000
H	3.59850000	4.76830000	1.08990000
C	5.56600000	4.88370000	1.62090000
C	5.26210000	4.51940000	3.03340000
C	6.12350000	3.72560000	3.88240000
C	4.78890000	4.18810000	5.68310000
C	3.88380000	4.87320000	4.83820000
C	2.72830000	5.47080000	5.38810000
H	2.10650000	5.91730000	4.82550000

C	2.50830000	5.40360000	6.74600000
C	3.42080000	4.71310000	7.60130000
C	4.53750000	4.11220000	7.06850000
H	5.13990000	3.64440000	7.63510000
C	3.14630000	4.60930000	9.01470000
C	1.37240000	6.07000000	7.32740000

2 Supplemental Figures

2.1 Photophysical properties

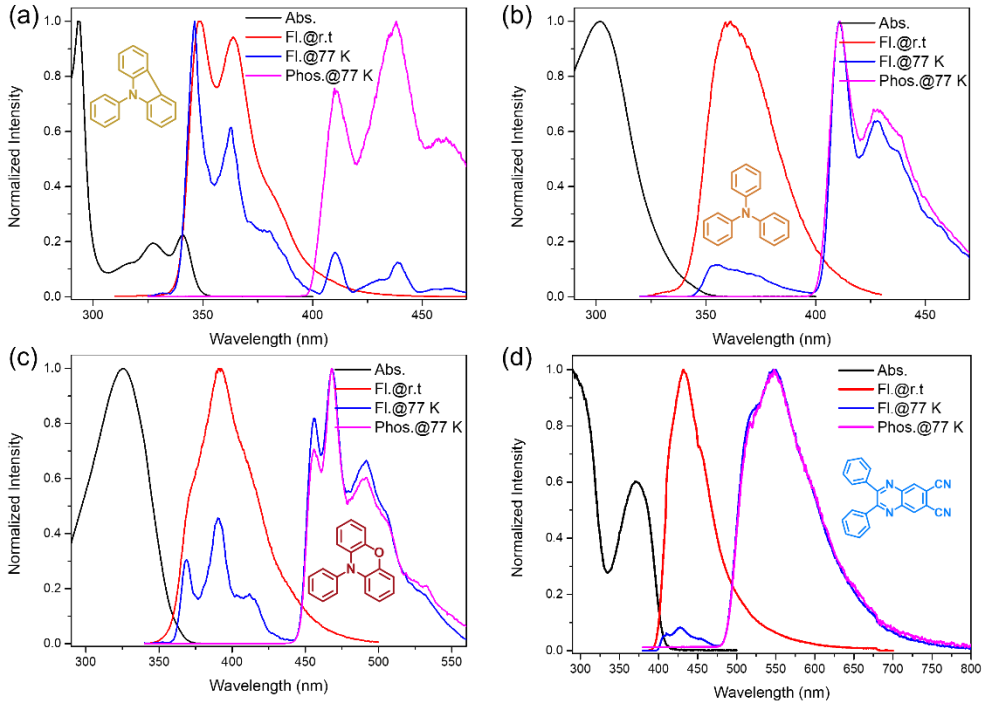

Figure S1. Absorption, fluorescence spectra measured at room temperature and fluorescence and phosphorescence spectra measured at 77K for (a) **Cz**, (b) **TPA**, (c) **PXZ**, and (d) **2CN**.

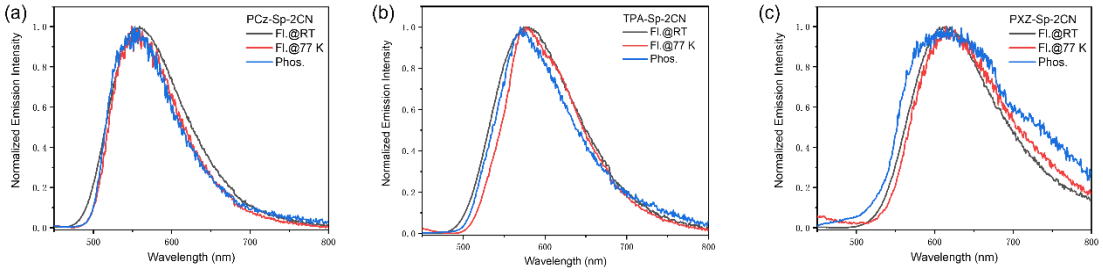

Figure S2. Room temperature fluorescence (Fl.@RT), low temperature fluorescence (Fl.@77 K), and low temperature phosphorescence (Phos.) of doped films of (a) **PCz-Sp-2CN**, (b) **TPA-Sp-2CN**, and (c) **PXZ-Sp-2CN** (3 wt% doped in CBP, 100 nm).

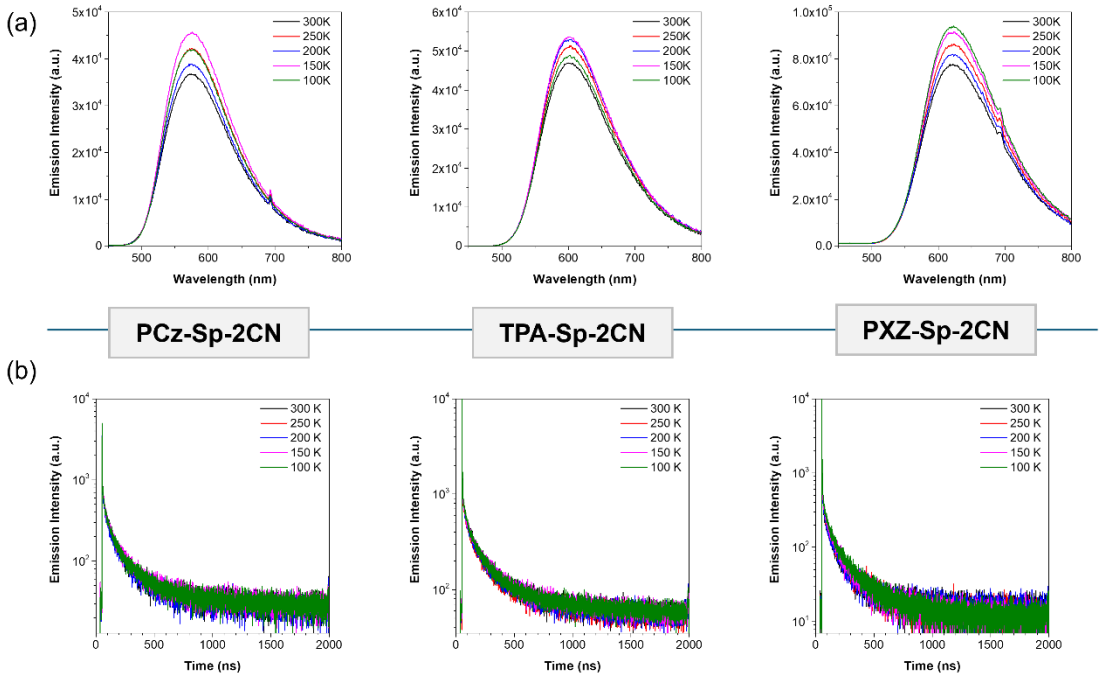

Figure S3. (a) Temperatures-dependent transient lifetimes and (b) temperature-dependent PL spectra of **PCz-Sp-2CN**, **TPA-Sp-2CN**, and **PXZ-Sp-2CN** in doped films.

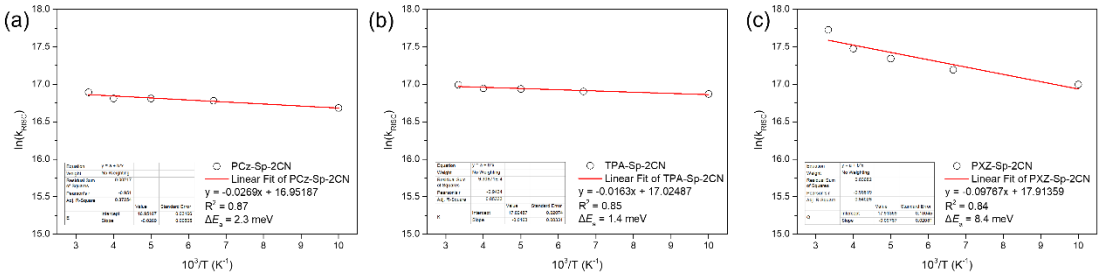

Figure S4. ln(K_{RISC}) were plotted as a function of 1000/T of doped (a) **PCz-Sp-2CN**, (b) **TPA-Sp-2CN**, and (c) **PXZ-Sp-2CN** films.

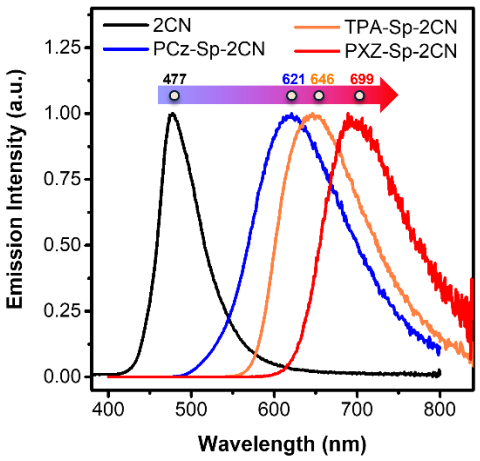

Figure S5. Fluorescence spectra of **2CN**, **PCz-Sp-2CN**, **TPA-Sp-2CN**, and **PXZ-Sp-2CN** solid powders.

2.2 Theoretical calculations

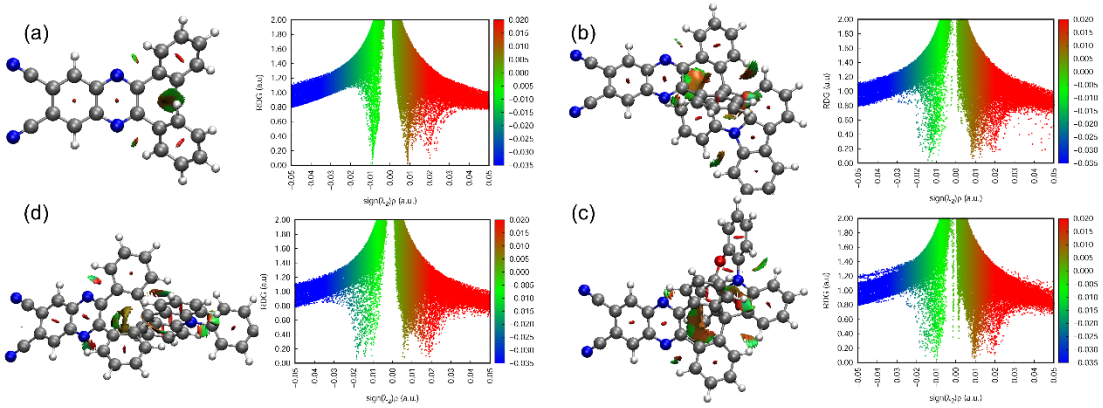

Figure S6. Reduced density gradient (RDG) iso-surface map with an iso-value of 0.5 and the functions of RDG and Sign(I_2)r for (a) **2CN**, (b) **PCz-Sp-2CN**, (c) **TPA-Sp-2CN**, and (d) **PXZ-Sp-2CN**.

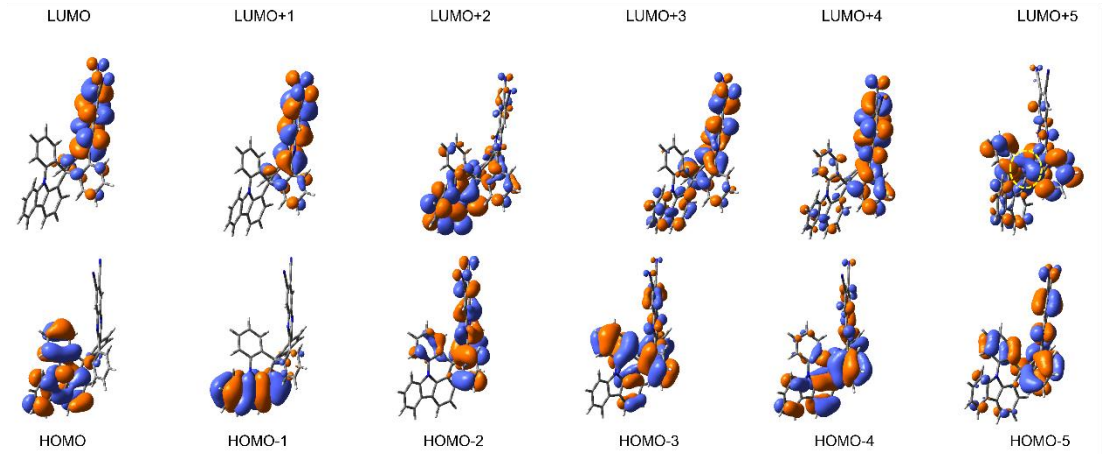

Figure S7. Molecular orbital amplitude plots of HOMO-5, HOMO-4, HOMO-3, HOMO-2, HOMO-1, HOMO, LUMO, LUMO+1, LUMO+2, LUMO+3, LUMO+4 and LUMO+5 of **PCz-Sp-2CN**. The yellow circle indicates the spatial orbital overlap of the fragments.

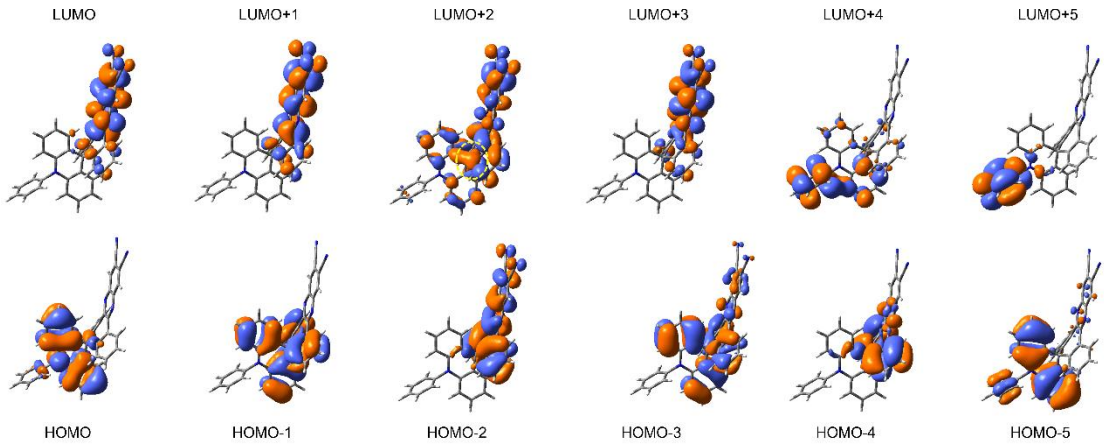

Figure S8. Molecular orbital amplitude plots of HOMO-5, HOMO-4, HOMO-3, HOMO-2, HOMO-1, HOMO, LUMO, LUMO+1, LUMO+2, LUMO+3, LUMO+4 and LUMO+5 of

TPA-Sp-2CN. The yellow circle indicates the spatial orbital overlap of the fragments.

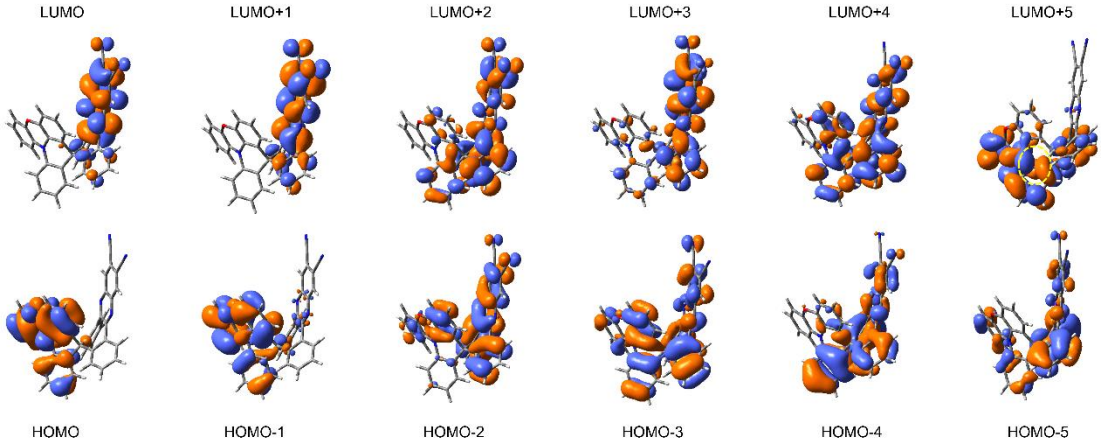

Figure S9. Molecular orbital amplitude plots of HOMO-5, HOMO-4, HOMO-3, HOMO-2, HOMO-1, HOMO, LUMO, LUMO+1, LUMO+2, LUMO+3, LUMO+4 and LUMO+5 of **PXZ-Sp-2CN**. The yellow circle indicates the spatial orbital overlap of the fragments.

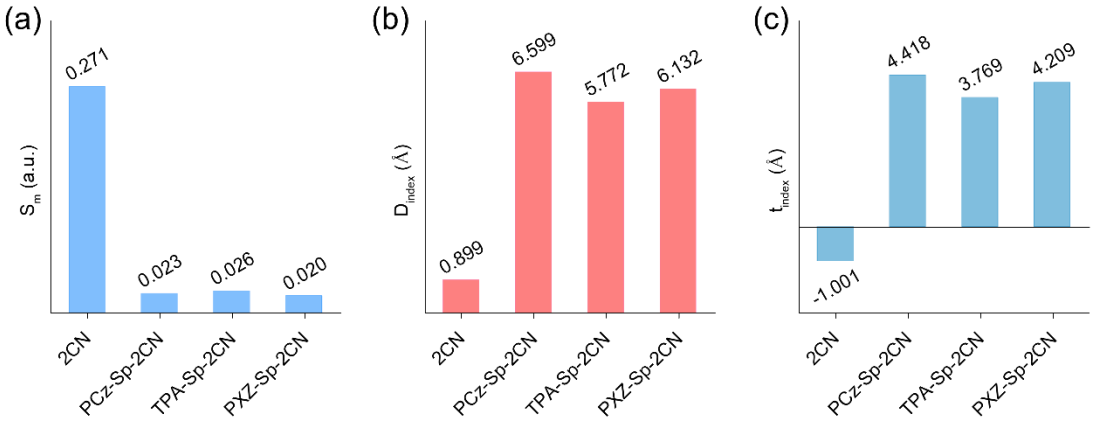

Figure S10. Quantitative description of the distribution characteristics of holes and electrons in space. S_m refers to the function of the overlap between the distribution of electrons and holes. The larger the index, the higher the overlap between holes and electrons; the smaller the value, the more significant the separation between holes and electrons. D_{index} refers to the index that measures the distance between the center of mass of holes and electrons. The larger the D_{index}, the more obvious the unidirectional charge transfer excitation. t_{index} refers to the degree of separation between holes and electrons. If the $t_{index} > 0$, it means that the separation of holes and electrons is relatively sufficient due to CT; if the $t_{index} < 0$, it means that there is no significant separation between holes and electrons in the CT direction.

2.3 Thermal properties

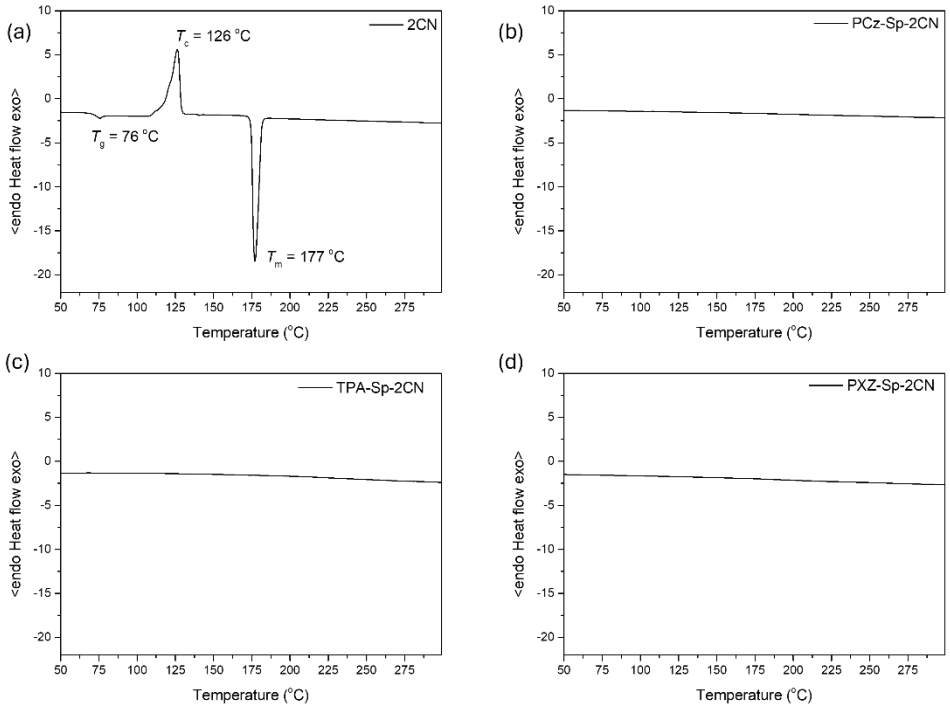

Figure S11. DSC curves of **2CN**, **PCz-Sp-2CN**, **TPA-Sp-2CN**, and **PXZ-Sp-2CN**.

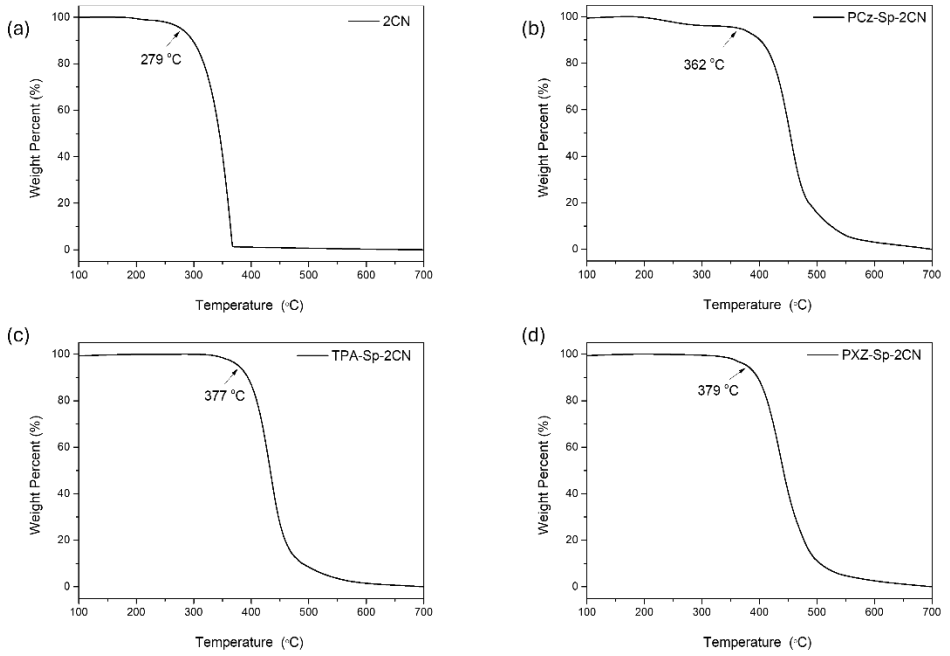

Figure S12. TGA curves of **2CN**, **PCz-Sp-2CN**, **TPA-Sp-2CN**, and **PXZ-Sp-2CN**.

2.4 Electrochemical properties

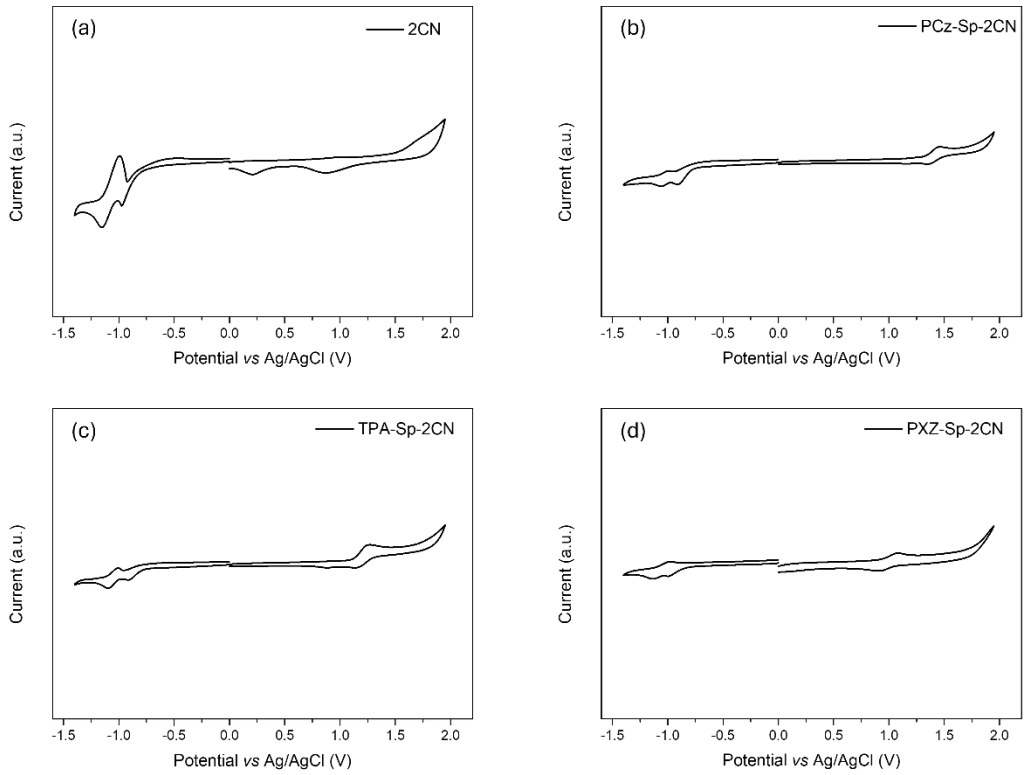

Figure S13. CV curves of **2CN**, **PCz-Sp-2CN**, **TPA-Sp-2CN**, and **PXZ-Sp-2CN**.

2.5 Device performance

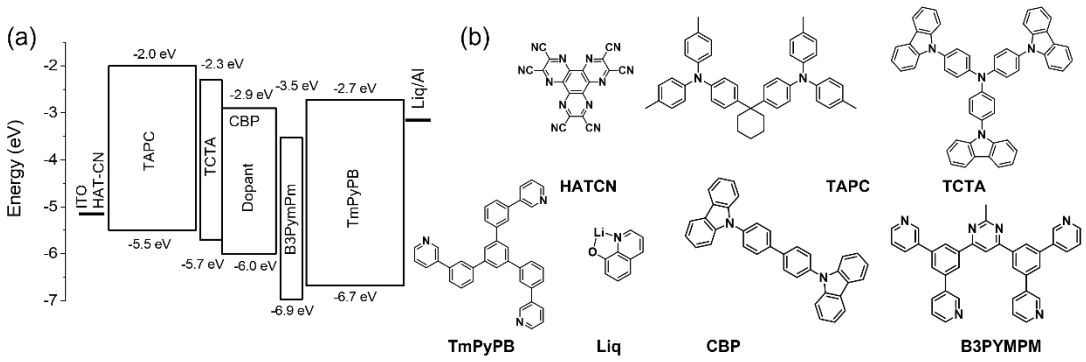

Figure S14. (a) Energy level diagrams of **PCz-Sp-2CN**, **TPA-Sp-2CN**, and **PXZ-Sp-2CN**-based devices as well as (b) molecular structures of the used materials.

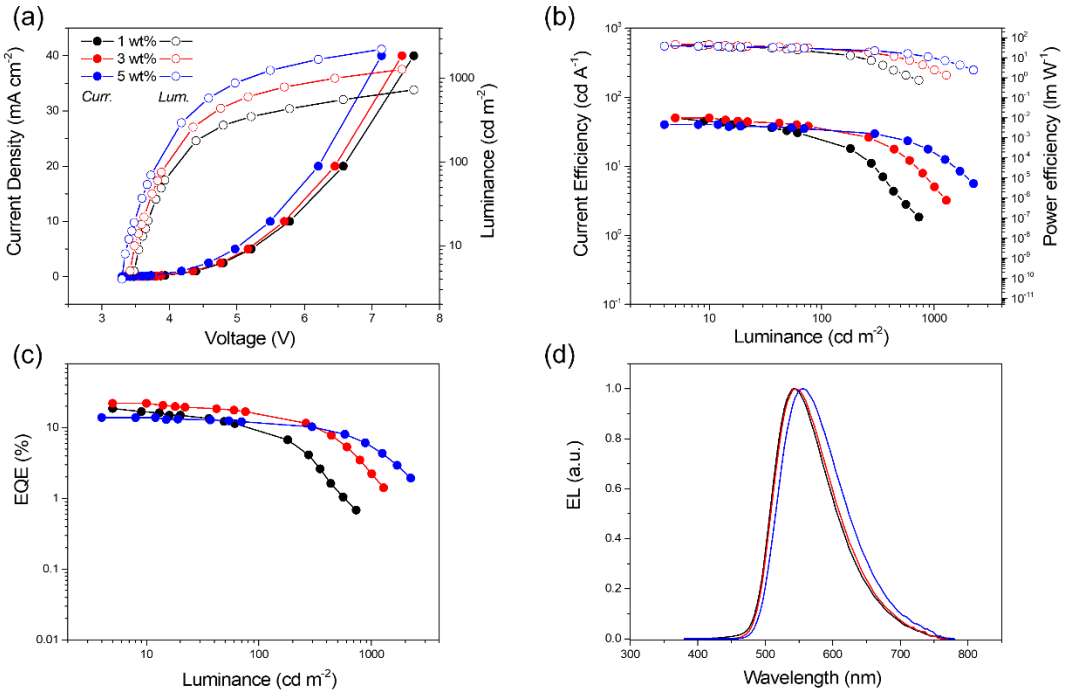

Figure S15. (a) The current density–voltage-luminance (*J*-V-L) characteristics of **PCz-Sp-2CN** doped devices at different dopant concentrations. (b) The current efficiency-luminance-power efficiency (CE-L-PE) characteristics of **PCz-Sp-2CN** doped devices at different dopant concentrations. (c) The external quantum efficiency versus luminance (EQE-L) curves of **PCz-Sp-2CN** doped devices at different dopant concentrations. (d) The normalized EL spectra at 10 mA cm^{-2}.

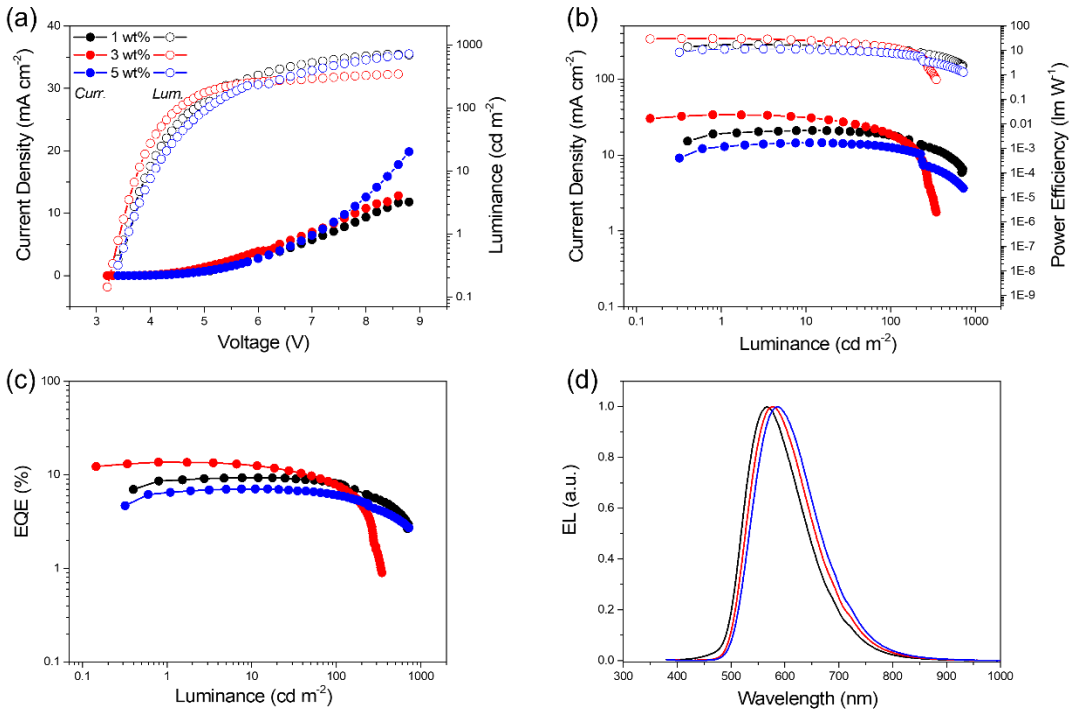

Figure S16. (a) The current density–voltage-luminance (*J*-V-L) characteristics of **TPA-Sp-2CN** doped devices at different dopant concentrations. (b) The current efficiency-luminance-power

efficiency (CE-L-PE) characteristics of **TPA-Sp-2CN** doped devices at different dopant concentrations. (c) The external quantum efficiency versus luminance (EQE-L) curves of **TPA-Sp-2CN** doped devices at different dopant concentrations. (d) The normalized EL spectra at 10 mA cm^{-2}.

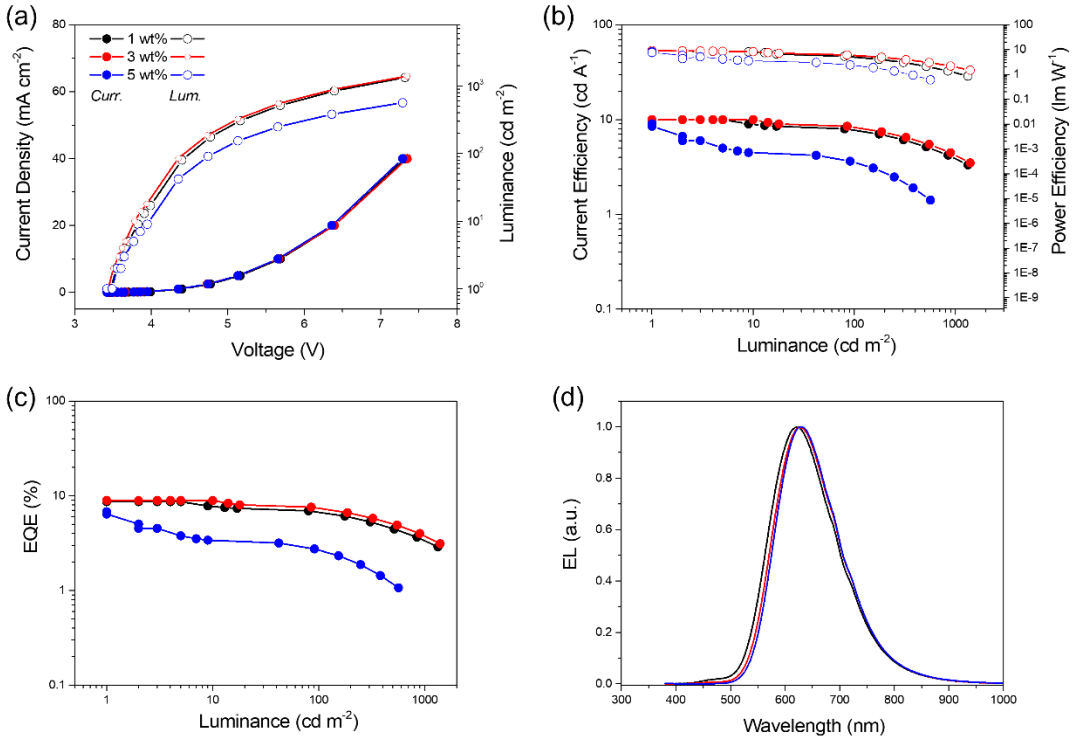

Figure S17. (a) The current density–voltage-luminance (*J*-V-L) characteristics of **PXZ-Sp-2CN** doped devices at different dopant concentrations. (b) The current efficiency-luminance-power efficiency (CE-L-PE) characteristics of **PXZ-Sp-2CN** doped devices at different dopant concentrations. (c) The external quantum efficiency versus luminance (EQE-L) curves of **PXZ-Sp-2CN** doped devices at different dopant concentrations. (d) The normalized EL spectra at 5 mA cm^{-2}.

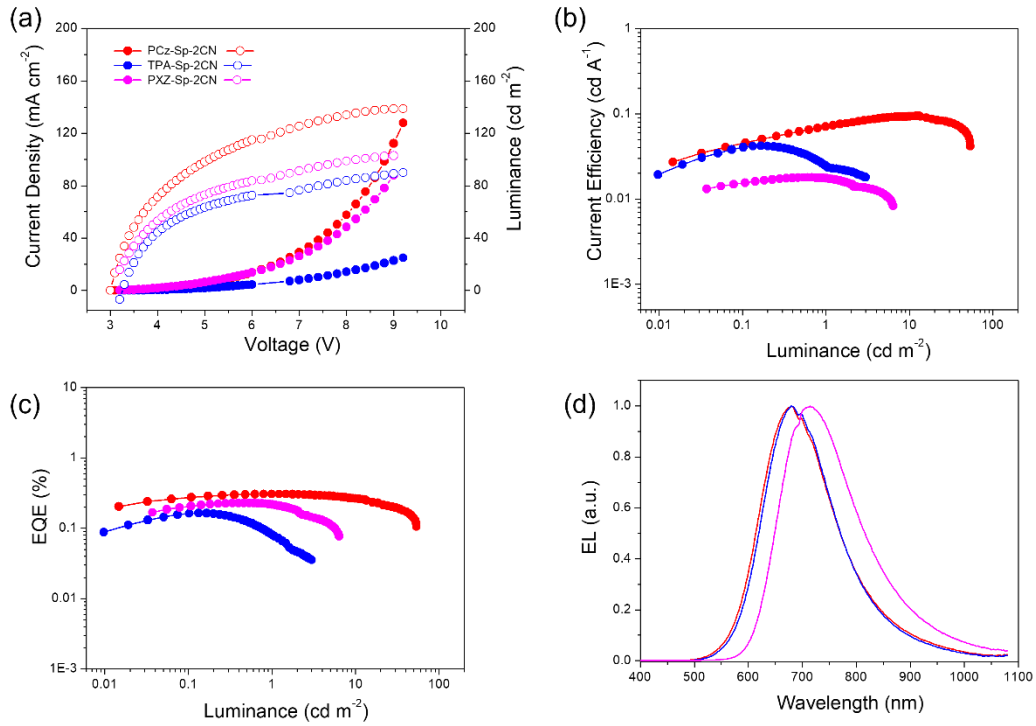

Figure S18. (a) The current density–voltage-luminance (*J*-V-L) characteristics of **PCz-Sp-2CN-**, **TPA-Sp-2CN-**, and **PXZ-Sp-2CN**-non-doped devices. (b) The current efficiency-luminance-power efficiency (CE-L-PE) characteristics of **PCz-Sp-2CN-**, **TPA-Sp-2CN-**, and **PXZ-Sp-2CN**-non-doped devices. (c) The external quantum efficiency versus luminance (EQE-L) curves of **PCz-Sp-2CN-**, **TPA-Sp-2CN-**, and **PXZ-Sp-2CN**-non-doped devices. (d) The normalized EL spectra at 5 mA cm^{-2}.

3 Supplemental Tables

3.1 Crystal data and structure refinement

Table S1. Crystal data and structure refinement for **9**.

Empirical formula	$C_{33}H_{19}NO_3$
Formula weight	477.49
Temperature/K	100
Crystal system	triclinic
Space group	P-1
Unit cell dimensions	a/Å: 9.7094(5) b/Å: 10.2557(5) c/Å: 12.1003(6) α/°: 105.243(2) β/°: 107.468(2) γ/°: 93.009(2)
Volume/ $Å^3$	1097.55(10)
Z	2
Density/g/cm^3	1.445
Absorption coefficient/mm^{-1}	0.093
F(000)	496.0
Crystal size/mm^3	0.12 × 0.06 × 0.04
Theta range for data collection/ °	4.444 to 52.93
Index ranges	-12 ⩽ h ⩽ 12 -12 ⩽ k ⩽ 12 -15 ⩽ l ⩽ 13
Reflections collected	10940
Independent reflections	4317 [R_{int} = 0.0432, R_{sigma} = 0.0658]
Data/restraints/parameters	4317/0/334
Goodness-of-fit on F^2	1.123
Final R indices [I>2sigma(I)]	R_1 = 0.0722, wR_2 = 0.1785
R indices (all data)	R_1 = 0.1204, wR_2 = 0.2440
Largest diff. peak and hole	0.58/-0.62
CCDC number	2435146
Radiation	MoKα (λ = 0.71073)

Table S2. Crystal data and structure refinement for **2CN**.

Empirical formula	$C_{22}H_{12}N_4$
Formula weight	332.36
Temperature/K	100.01(10)
Crystal system	monoclinic
Space group	$P2_1/n$
Unit cell dimensions	a/Å: 11.37795(11) b/Å: 7.57095(7) c/Å: 39.0727(3) α/°: 90 β/°: 94.7078(9) γ/°: 90
Volume/ $Å^3$	3354.44(5)
Z	8
Density/g/cm^3	1.316
Absorption coefficient/mm^{-1}	0.639
F(000)	1376.0
Crystal size/mm^3	0.4 × 0.35 × 0.3
Theta range for data collection/ °	9.084 to 149.356
Index ranges	-13 ⩽ h ⩽ 14 -9 ⩽ k ⩽ 9 -32 ⩽ l ⩽ 48
Reflections collected	20071
Independent reflections	6720 [R_{int} = 0.0197, R_{sigma} = 0.0190]
Data/restraints/parameters	6720/171/524
Goodness-of-fit on F^2	1.021
Final R indices [I>2sigma(I)]	R_1 = 0.0338, wR_2 = 0.0839
R indices (all data)	R_1 = 0.0384, wR_2 = 0.0872
Largest diff. peak and hole	0.24/-0.18
CCDC number	2238546
Radiation	Cu Kα (λ = 1.54184)

Table S3. Crystal data and structure refinement for **PCz-Sp-2CN**.

Empirical formula	$C_{41}H_{21}N_5$
Formula weight	583.63
Temperature/K	100.01(10)
Crystal system	triclinic
Space group	P-1
Unit cell dimensions	a/Å: 8.5364(4) b/Å: 13.0640(5) c/Å: 13.1415(6) α/°: 78.073(4) β/°: 84.390(4) γ/°: 76.421(4)
Volume/ $Å^3$	1391.95(11)
Z	2
Density/g/cm^3	1.392
Absorption coefficient/mm^{-1}	0.656
F(000)	604.0
Crystal size/mm^3	0.16 × 0.16 × 0.15
Theta range for data collection/ °	6.884 to 153.934
Index ranges	-9 ⩽ h ⩽ 10 -16 ⩽ k ⩽ 14 -16 ⩽ l ⩽ 16
Reflections collected	10712
Independent reflections	5748 [R_{int} = 0.0148, R_{sigma} = 0.0213]
Data/restraints/parameters	5748/0/416
Goodness-of-fit on F^2	1.035
Final R indices [I>2sigma(I)]	R_1 = 0.0413, wR_2 = 0.1033
R indices (all data)	R_1 = 0.0454, wR_2 = 0.1067
Largest diff. peak and hole	0.37/-0.21
CCDC number	2238547
Radiation	Cu Kα (λ = 1.54184)

Table S4. Crystal data and structure refinement for **TPA-Sp-2CN**.

Empirical formula	$C_{41}H_{23}N_5$
Formula weight	585.64
Temperature/K	100(1)
Crystal system	orthorhombic
Space group	Pbca
Unit cell dimensions	a/Å: 12.05609(8) b/Å: 14.50624(10) c/Å: 32.9900(2) α/°: 90 β/°: 90 γ/°: 90
Volume/ $Å^3$	5769.57(6)
Z	8
Density/g/cm^3	1.348
Absorption coefficient/mm^{-1}	0.633
F(000)	2432.0
Crystal size/mm^3	0.3 × 0.2 × 0.18
Theta range for data collection/ °	9.086 to 154.596
Index ranges	-15 ⩽ h ⩽ 12 -18 ⩽ k ⩽ 15 -41 ⩽ l ⩽ 41
Reflections collected	36705
Independent reflections	6074 [R_{int} = 0.0220, R_{sigma} = 0.0136]
Data/restraints/parameters	6074/0/416
Goodness-of-fit on F^2	1.029
Final R indices [I>2sigma(I)]	R_1 = 0.0336, wR_2 = 0.0824
R indices (all data)	R_1 = 0.0365, wR_2 = 0.0848
Largest diff. peak and hole	0.27/-0.18
CCDC number	2223305
Radiation	Cu Kα (λ = 1.54184)

Table S5. Crystal data and structure refinement for **PXZ-Sp-2CN**.

Empirical formula	$C_{41}H_{21}N_5O$
Formula weight	599.63
Temperature/K	99.97(10)
Crystal system	triclinic
Space group	P-1
Unit cell dimensions	a/Å: 14.7786(5) b/Å: 15.3778(4) c/Å: 16.3190(5) α/°: 62.436(3) β/°: 66.796(3) γ/°: 72.923(3)
Volume/ $Å^3$	2993.46(18)
Z	4
Density/g/cm^3	1.331
Absorption coefficient/mm^{-1}	0.651
F(000)	1240.0
Crystal size/mm^3	0.16 × 0.15 × 0.15
Theta range for data collection/ °	6.414 to 153.914
Index ranges	-18 ⩽ h ⩽ 17 -18 ⩽ k ⩽ 13 -20 ⩽ l ⩽ 17
Reflections collected	20019
Independent reflections	12106 [R_{int} = 0.0189, R_{sigma} = 0.0273]
Data/restraints/parameters	12106/354/973
Goodness-of-fit on F^2	1.071
Final R indices [I>2sigma(I)]	R_1 = 0.0471, wR_2 = 0.1106
R indices (all data)	R_1 = 0.0523, wR_2 = 0.1139
Largest diff. peak and hole	0.26/-0.31
CCDC number	2239664
Radiation	CuKα (λ = 1.54184)

3.2 Photophysical information

Table S6. The various rate constants for **PCz-Sp-2CN**, **TPA-Sp-2CN**, and **PXZ-Sp-2CN**.

Compound	κ_{PF} (10^6 s^{-1}) [a]	κ_{IC} (10^6 s^{-1}) [a]	κ_{ISC} (10^6 s^{-1}) [a]	κ_{RISC} (10^6 s^{-1}) [a]
PCz-Sp-2CN	9.32	0.19	22.50	5.15
TPA-Sp-2CN	4.13	2.42	22.40	1.79
PXZ-Sp-2CN	12.20	8.12	101.00	2.81

Conditions: [a] The data were obtained based on the transient photoluminescence lifetime and PLQY of the doped films. Where κ_{PF} is the radiative decay rate for prompt fluorescence; κ_{IC}, κ_{ISC} and κ_{RISC} are the internal conversion, intersystem crossing and reverse intersystem crossing rate constants, respectively.

3.3 Theoretical calculations

Table S7. Theoretical Calculation Data of **2CN**, **PCz-Sp-2CN**, **TPA-Sp-2CN**, and **PXZ-Sp-2CN**.

Compound	S_1 (eV)	T_1 (eV)	ΔE_{ST} (eV)	f	$\langle T_1\|H_{SO}\|S_1\rangle$ (cm^{-1})
2CN	2.713	2.183	0.530	0.2930	6.83
PCz-Sp-2CN	2.029	1.947	0.082	0.0198	0.21
TPA-Sp-2CN	1.794	1.734	0.060	0.0559	0.13
PXZ-Sp-2CN	1.488	1.446	0.042	0.0027	0.06

Conditions: Time-dependent density-functional theory based on PBE0 functional with the def2-TZVP basis set. The spin–orbit coupling constants ($\langle T_1|H_{SO}|S_1\rangle$) as well as the energy gap between S_1 and T_1 (ΔE_{ST}). f is the vibration strength of the molecule.

3.4 The device performance

Table S8. Electroluminescence characteristics of the **PCz-Sp-2CN** doped devices at different dopant concentrations.

PCz-Sp-2CN	V [a] (V)	CE [b] (cd A^{-1})	PE [b] (lm W^{-1})	EQE [b] (%)	λ_{EL} [c] (nm)	FWHM [c] (nm)	CIE [c] (x, y)
1 wt%	3.48	50.0/23.4	45.2/17.7	18.7/9.1	540	100	0.40,0.56
3 wt%	3.42	50.0/35.1	45.9/27.6	22.1/15.5	544	102	0.41,0.56
5 wt%	3.30	40.0/33.6	38.1/27.5	13.9/11.7	552	107	0.44, 0.54

[a] Recorded at a luminance of 0.01 mA cm^{-2}; [b] corresponded to the maximum value, and the value determined at the luminance of 100 cd m^{-2}; [c] determined from the EL spectra measured at a current density of 10 mA cm^{-2}.

Table S9. Electroluminescence characteristics of the **TPA-Sp-2CN** doped devices at different dopant concentrations.

TPA-Sp-2CN	V [a] (V)	CE[b] (cd A^{-1})	PE [b] (lm W^{-1})	EQE[b] (%)	λ_{EL} [c] (nm)	FWHM [c] (nm)	CIE [c] (x, y)
1 wt%	3.68	21.0/18.9	17.3/14.4	9.3/8.6	566	125	0.46,0.51
3 wt%	3.58	33.9/18.5	31.3/14.5	13.7/7.8	578	130	0.49,0.50
5 wt%	3.63	14.5/12.4	11.5/8.5	7.1/6.1	586	133	0.51,0.48

[a] Recorded at a luminance of 0.01 mA cm^{-2}; [b] corresponded to the maximum value, and the value determined at the luminance of 100 cd m^{-2}; [c] determined from the EL spectra measured at a current density of 10 mA cm^{-2}.

Table S10. Electroluminescence characteristics of the **PXZ-Sp-2CN** doped devices at different dopant concentrations.

PXZ-Sp-2CN	V[a] (V)	CE[b] (cd A^{-1})	PE [b] (lm W^{-1})	EQE[b] (%)	λ_{EL} [c] (nm)	FWHM [c] (nm)	CIE [c] (x, y)
1 wt%	3.47	10.0/7.7	9.1/4.9	8.7/6.7	622	138	0.56, 0.42
3 wt%	3.44	10.0/8.3	9.6/6.3	9.0/7.4	626	135	0.58, 0.41
5 wt%	3.42	9.0/3.5	8.3/2.3	6.8/2.6	628	131	0.60, 0.40

[a] Recorded at a luminance of 0.01 mA cm^{-2}; [b] corresponded to the maximum value, and the value determined at the luminance of 100 cd m^{-2}; [c] determined from the EL spectra measured at a current density of 10 mA cm^{-2}.

Table S11. Electroluminescence characteristics of the **PCz-Sp-2CN-**, **TPA-Sp-2CN-**, and **PXZ-Sp-2CN**-non-doped devices

100 wt%	V[a] (V)	CE[b] (cd A^{-1})	PE [b] (lm W^{-1})	EQE[b] (%)	λ_{EL} [c] (nm)	FWHM [c] (nm)	CIE[c] (x, y)
PCz-Sp-2CN	3.1	0.09	0.06	0.31	680	156	0.64, 0.35
TPA-Sp-2CN	3.4	0.04	0.03	0.16	680	151	0.63, 0.36
PXZ-Sp-2CN	3.5	0.02	0.01	0.23	714	167	0.64, 0.36

[a] Recorded at a luminance of 0.1 mA cm^{-2}; [b] corresponded to the maximum value; [c] determined from the EL spectra measured at a current density of 10 mA cm^{-2}.

Table S12. EL performance of representative Spiro TSCT TADF OLEDs.

Compound	λ_{EL} (nm)	EQE (%)	REF.
1	490	22.6	[7]
2	470	9.4	[7]
3	466	7.4	[7]
SPS	520	8.5	[8]
SPO	528	17.8	[8]
SPON	552	14.4	[8]
AC-BO	456	19.3	[9]
QAC-BO	448	15.8	[9]
Cz-BO	412	5.5	[9]
1	494	20.9	[10]
2	527	16.1	[10]
3	503	17.7	[10]
4	507	20	[10]
5	550	13.2	[10]
1	512	21	[11]
2	513	23.1	[11]
3	521	18.6	[11]
2PXZ-2TRZ	508	27.1	[12]
DM-BD1	500	28	[13]
DM-BD2	500	26.6	[13]
C6-DMB	492	21	[14]
tBu-DMB	492	21.7	[14]
PhCzSpiroS-TRZ	490	33.6	[15]
2tDMG	504	30.8	[16]
3tDMG	518	26.3	[16]
DM-Me-B	500	19.2	[17]
STF-DBTS	488	10.3	[18]
DM-B	492	27.4	[19]
DM-Bm	500	21.7	[19]
DM-G	500	18.5	[19]
SFST	508	23.1	[20]
SFOT	508	12.5	[20]
SDMAC	492	28.4	[21]
SFO-SPAC	502	23.5	[22]
SFO-DMAC	532	15.6	[22]
dCz-Xo-TRZ	477	27.8	[23]
mCz-Xo-TRZ	464	21	[23]
8MeDM-B	492	28.8	[24]
8FDM-B	496	31.7	[24]
SIR-A	520	18.3	[25]
SIR-B	520	20.4	[25]

SIR-C	520	18.4	[25]
QAFCN	488	17.9	[26]
ACRFLCN	505	11.5	[26]
OSFSO	472	20	[27]
SAF-3CN	532	19.4	[28]
SCN	519	23	[29]
SPHCN	512	15.4	[29]
SCFPY	517	23.3	[29]
SAF36DCPP	604	16.1	[30]
SAF27DCPP	604	11.8	[30]
1	500	14.9	[31]
2	497	8	[31]
3	548	13.5	[31]
PCz-Sp-2CN	**544**	**22.1**	This work
TPA-Sp-2CN	**578**	**13.7**	This work
PXZ-Sp-2CN	**626**	**9.0**	This work
PCz-Sp-2CN	**680**	**0.31**	This work
TPA-Sp-2CN	**680**	**0.16**	This work
PXZ-Sp-2CN	**714**	**0.23**	This work

4 Copy of NMR Spectra and MALDI-TOF-MS Plot

4.1 ^{1}H NMR plot of 4, 400 MHz, $CDCl_3$

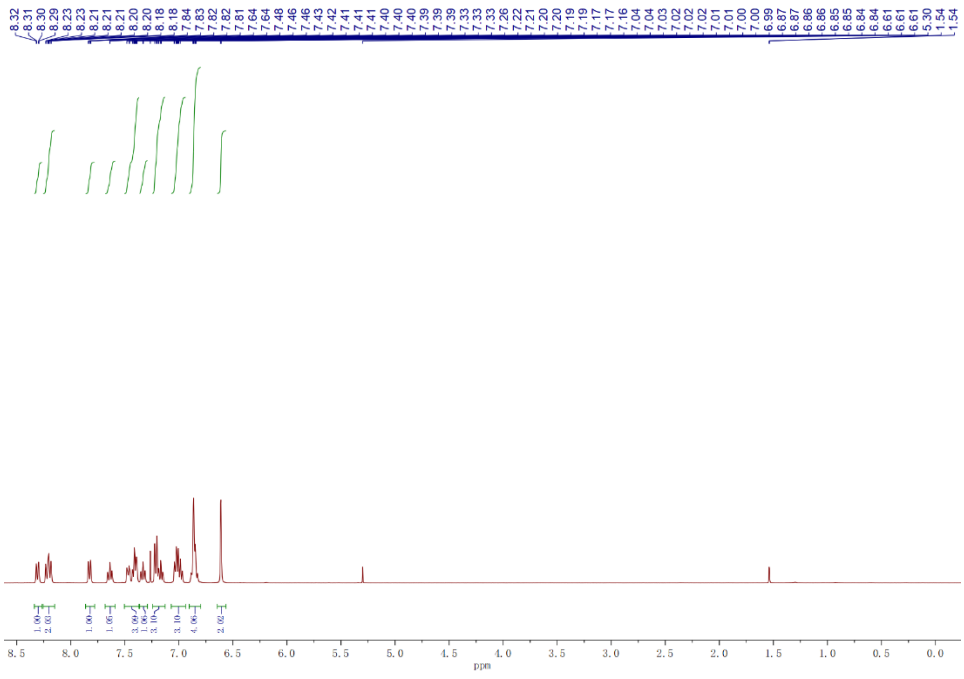

4.2 ^{13}C NMR plot of 4, 101 MHz, $CDCl_3$

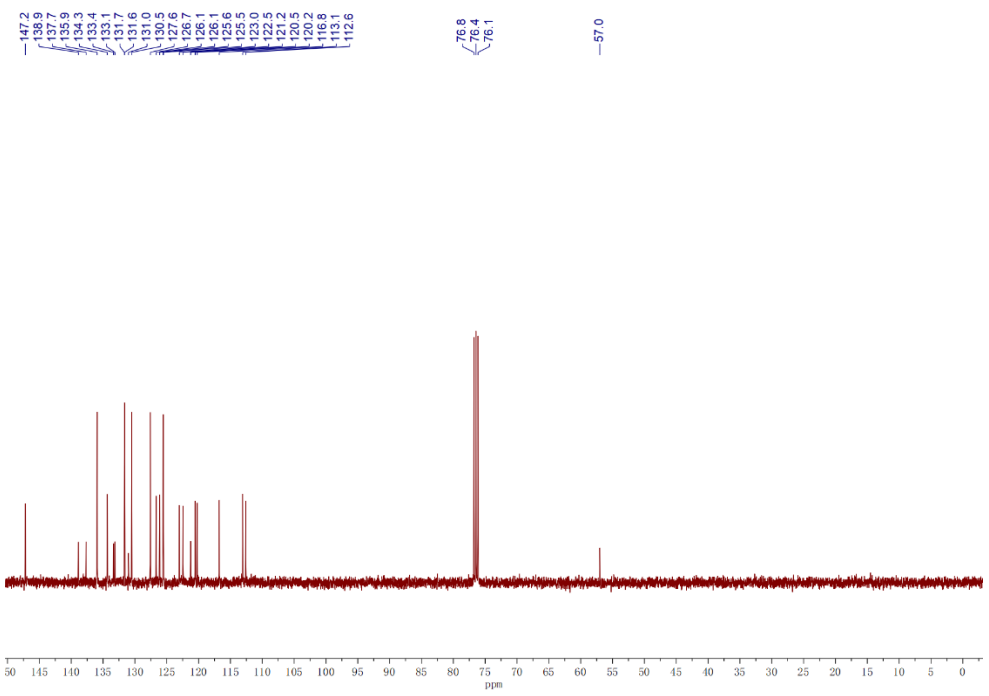

4.3 MALDI-MS (HRMS) plot of 4

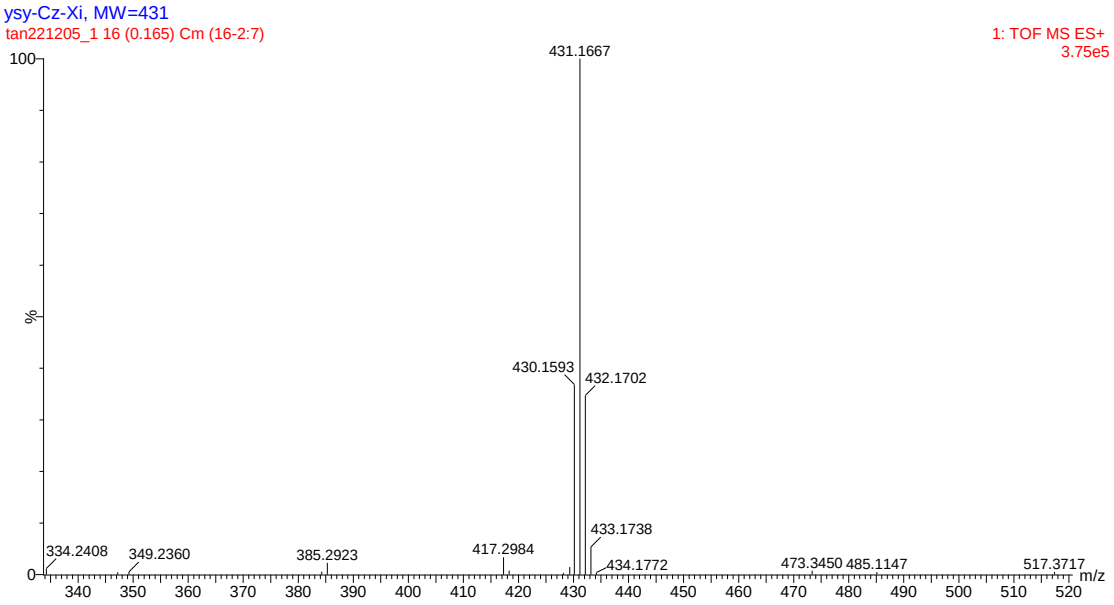

4.4 ^{1}H NMR plot of 5, 400 MHz, $CDCl_3$

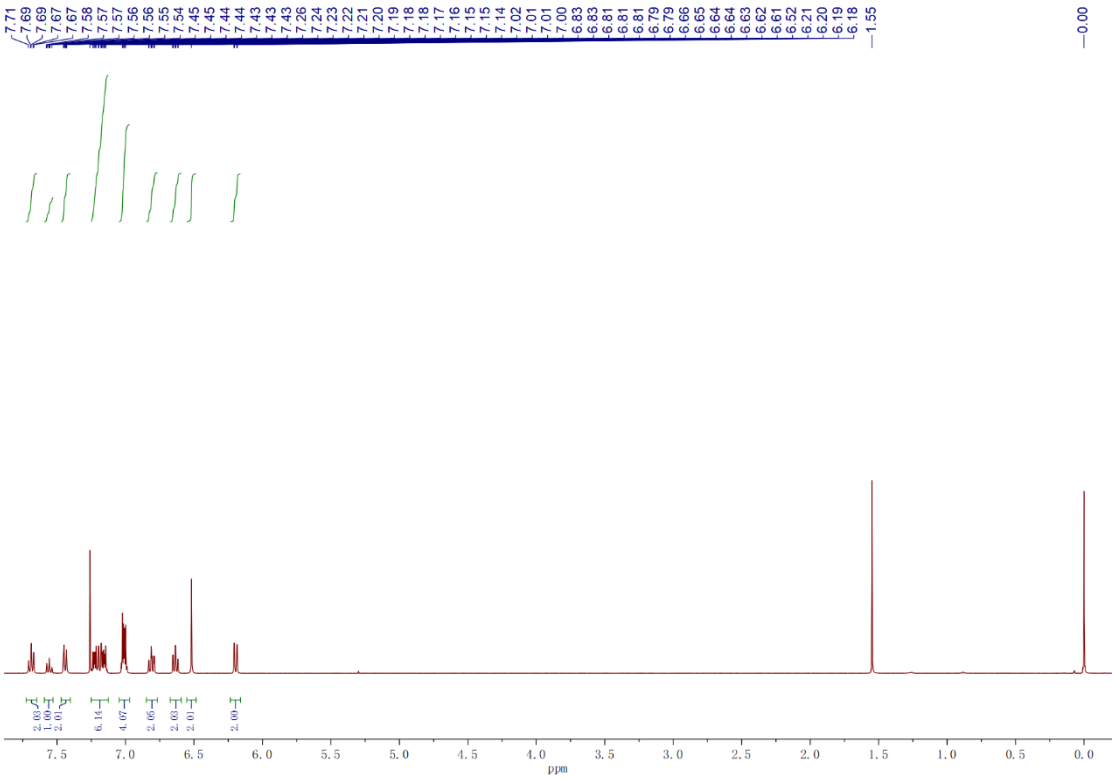

4.5 ^{13}C NMR plot of 5, 101 MHz, $CDCl_3$

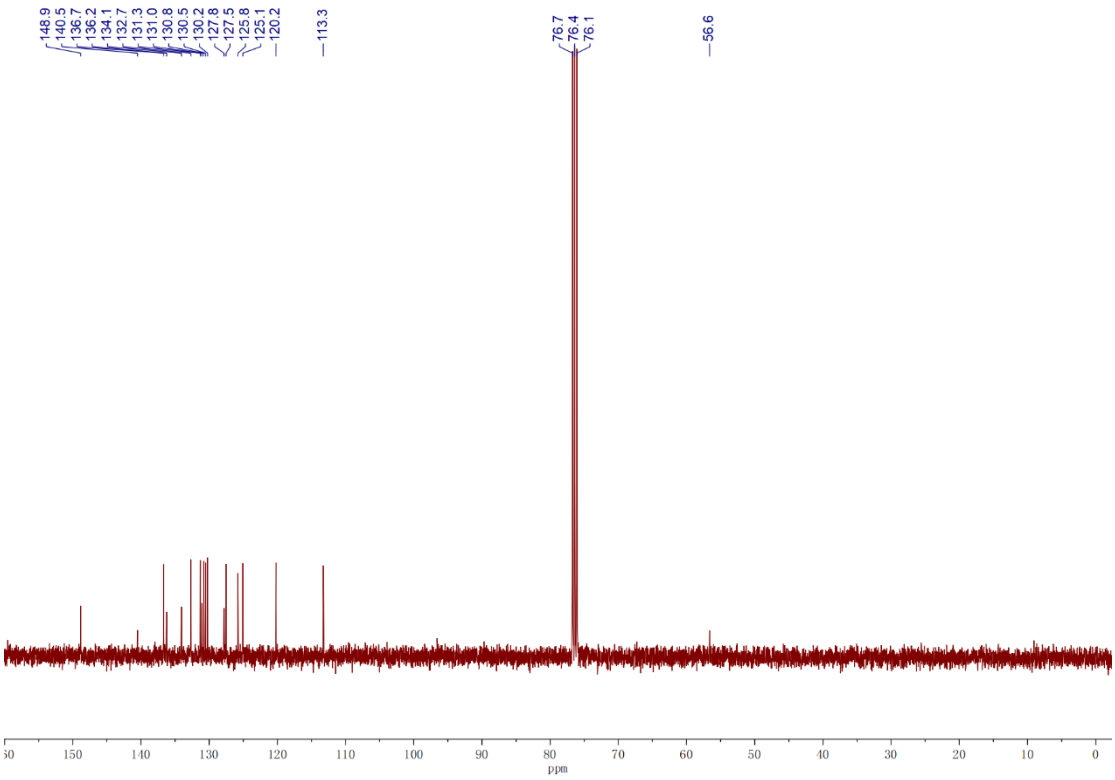

4.6 MALDI-MS (HRMS) plot of 5

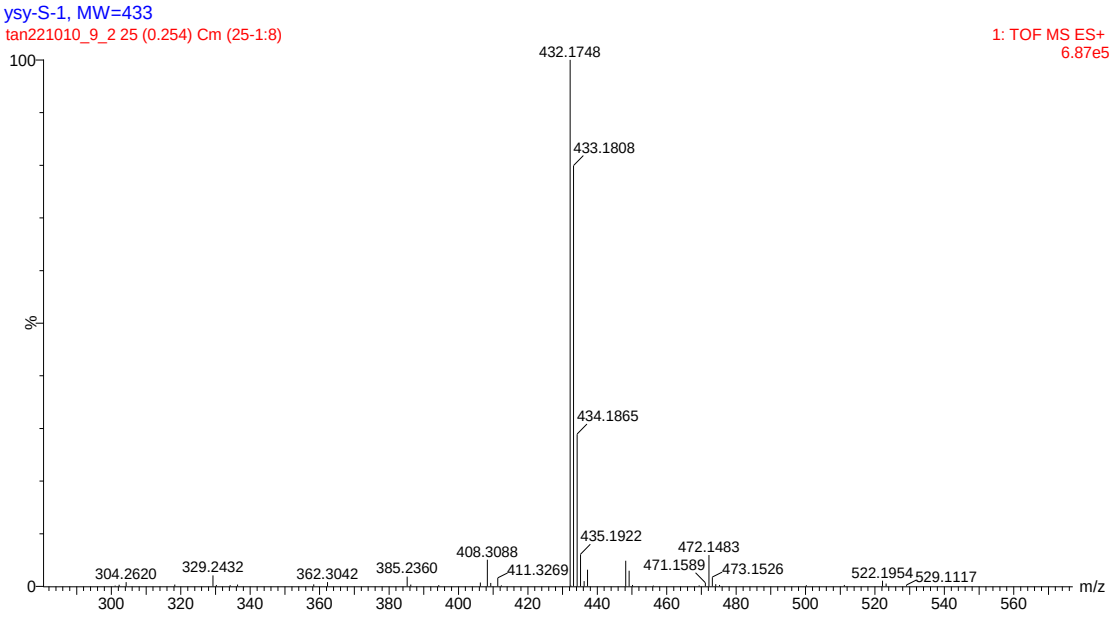

4.7 ^{1}H NMR plot of 6, 400 MHz, $CDCl_3$

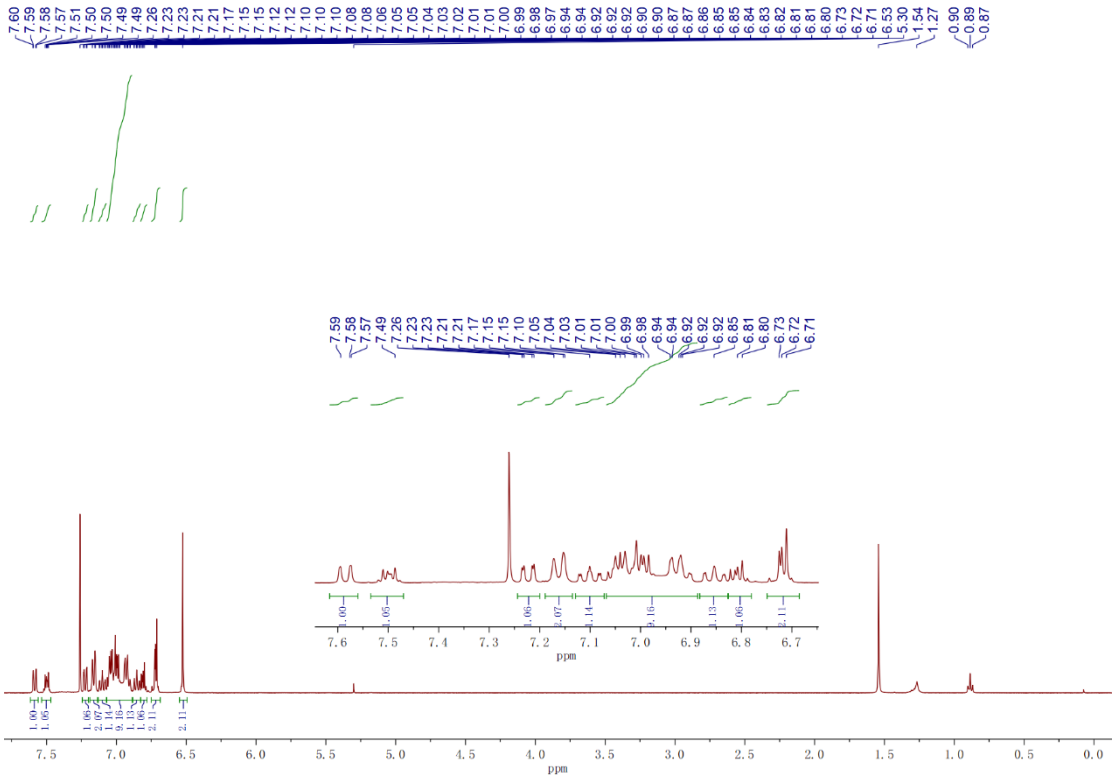

4.8 ^{13}C NMR plot of 6, 101 MHz, $CDCl_3$

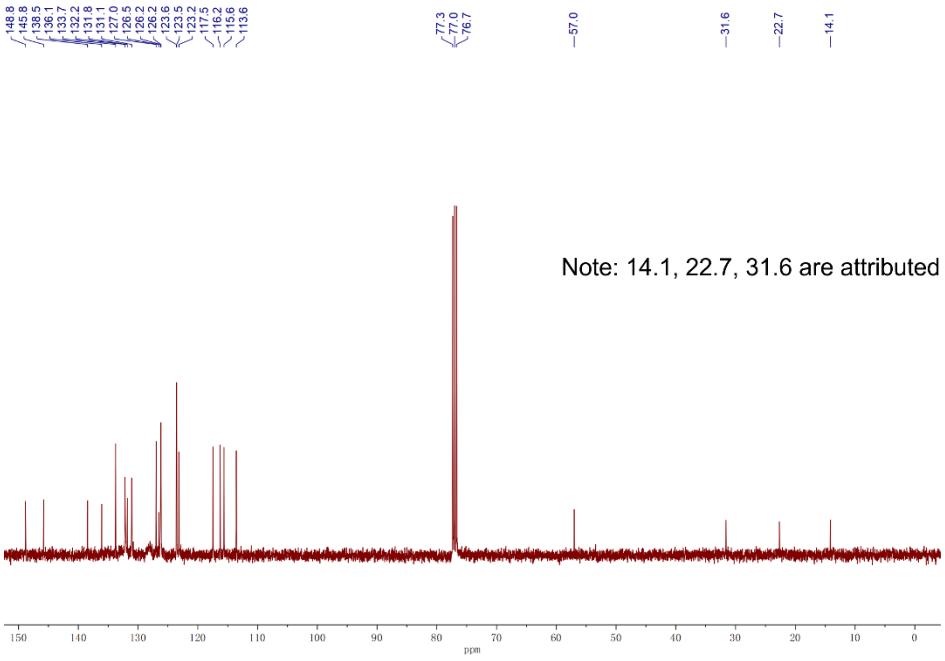

4.9 MALDI-MS (HRMS) plot of 6

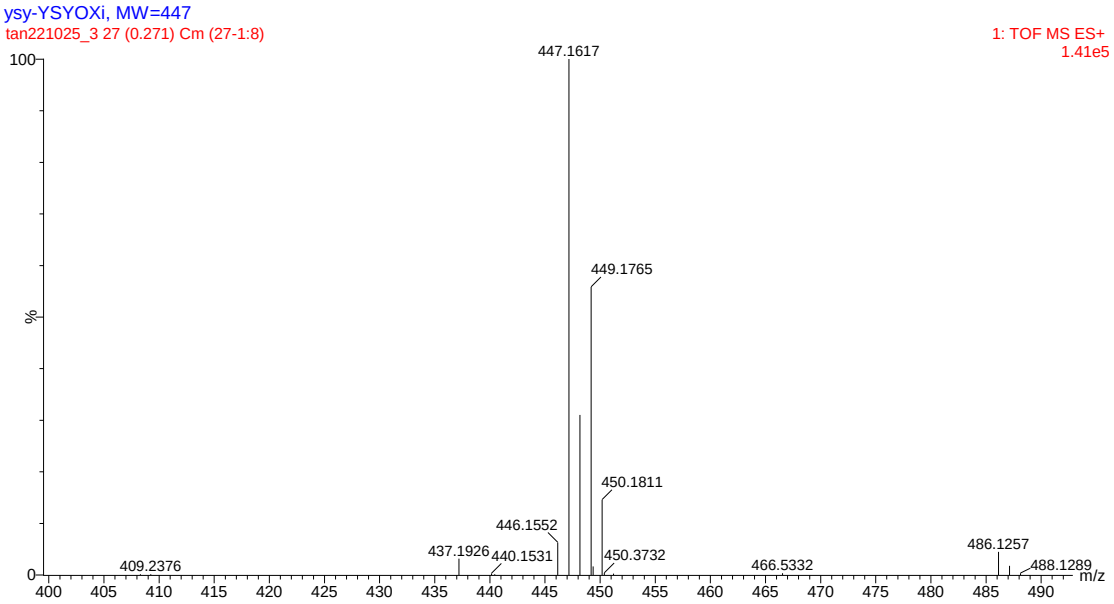

4.10 ^{1}H NMR plot of 7, 400 MHz, $CDCl_3$

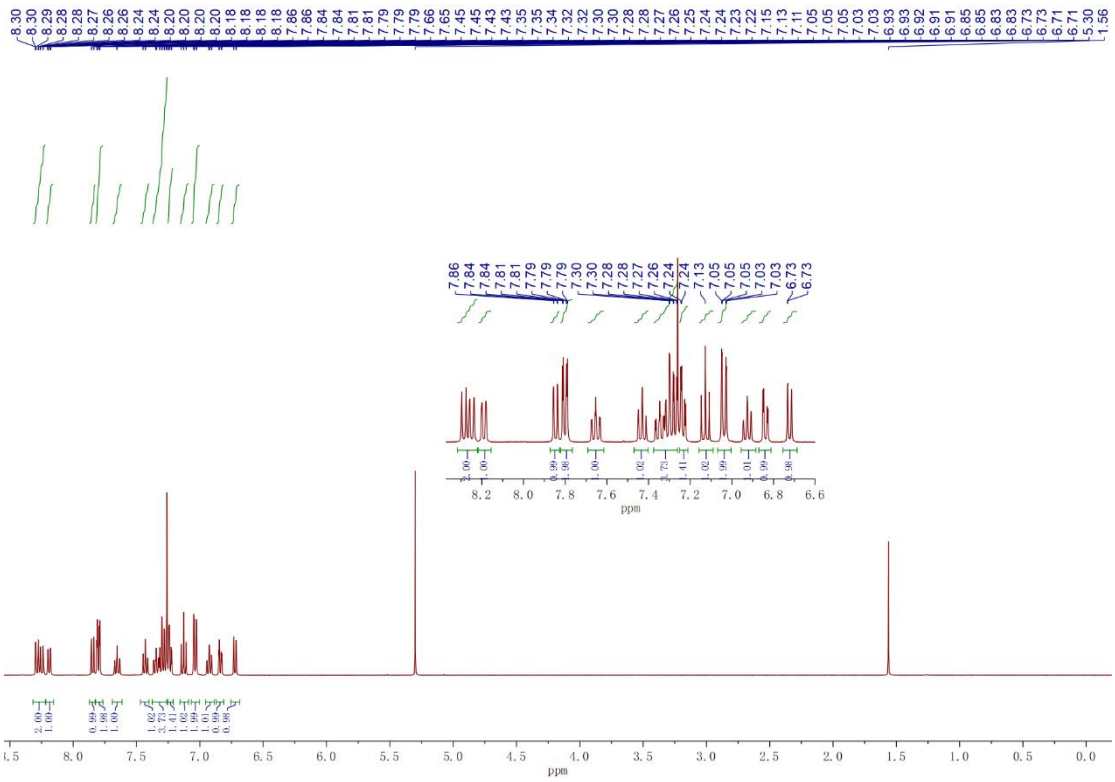

4.11 ^{13}C NMR plot of 7, 101 MHz, $CDCl_3$

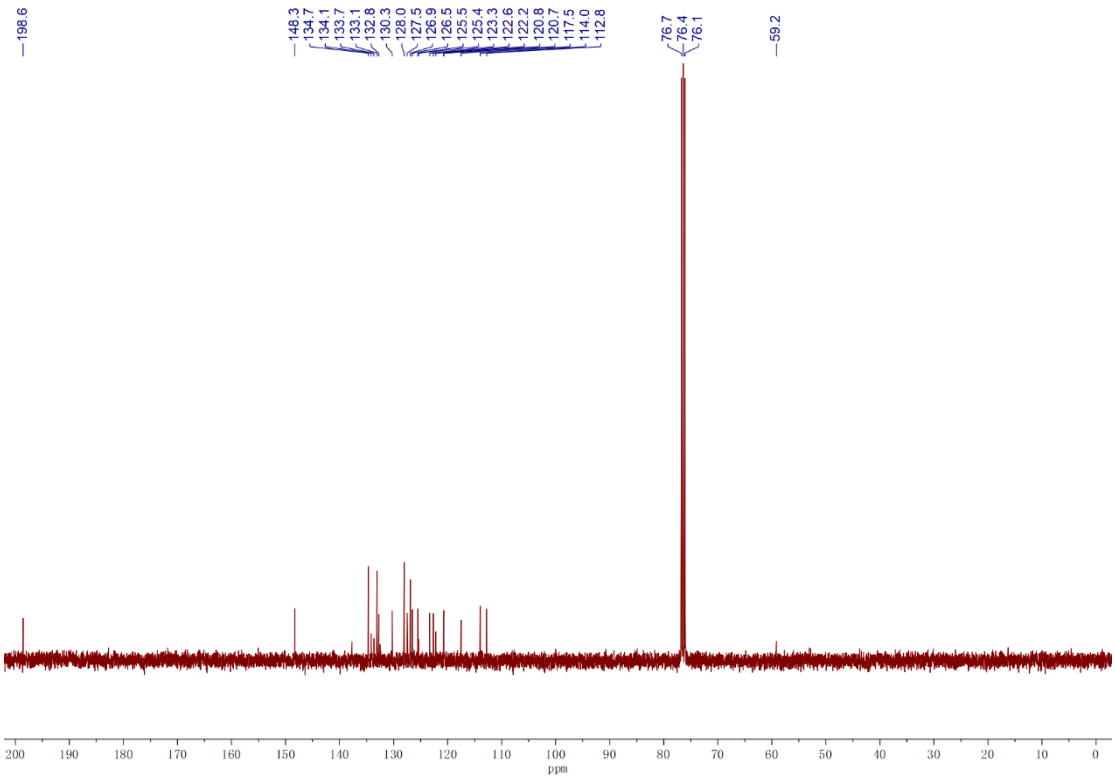

4.12 MALDI-MS (HRMS) plot of 7

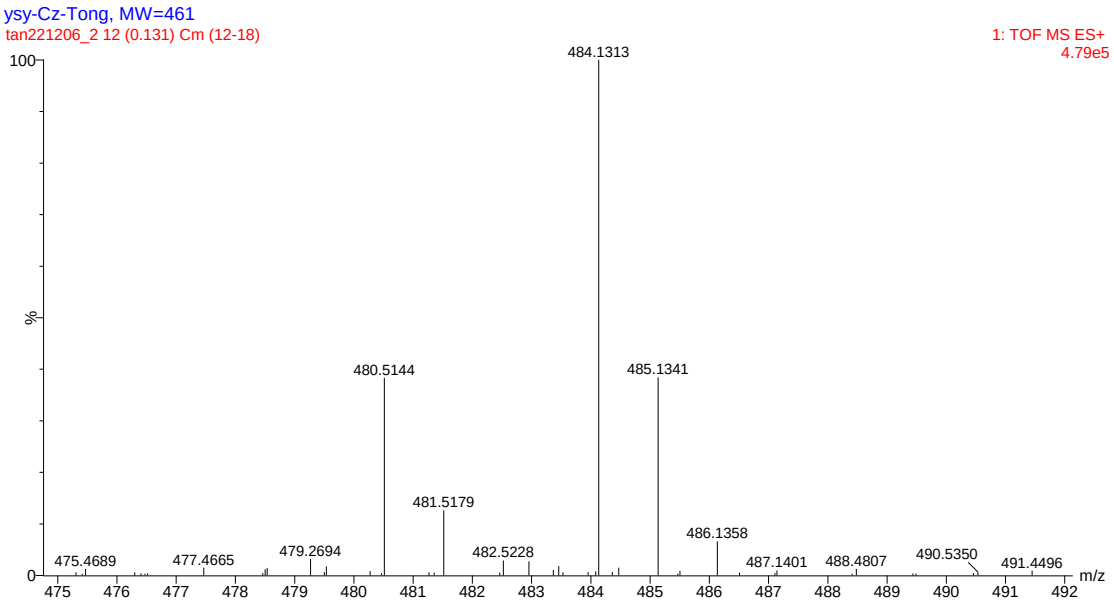

4.13 ^{1}H NMR plot of 8, 400 MHz, $CDCl_3$

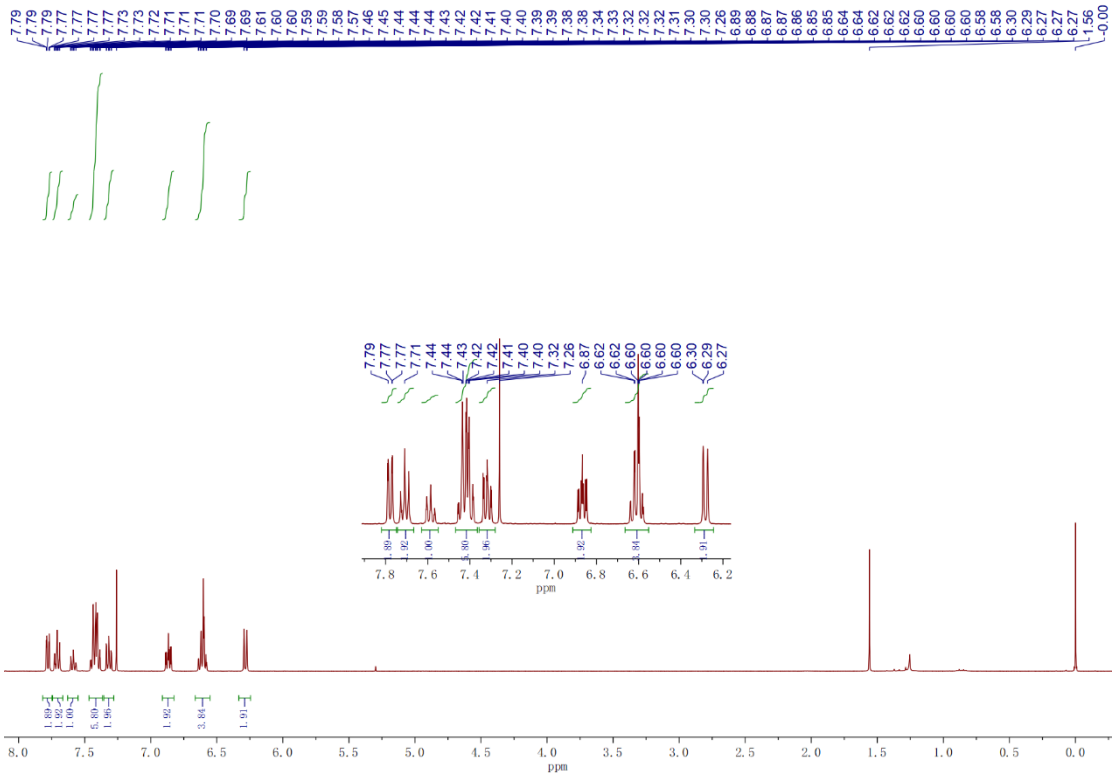

4.14 ^{13}C NMR plot of 8, 101 MHz, $CDCl_3$

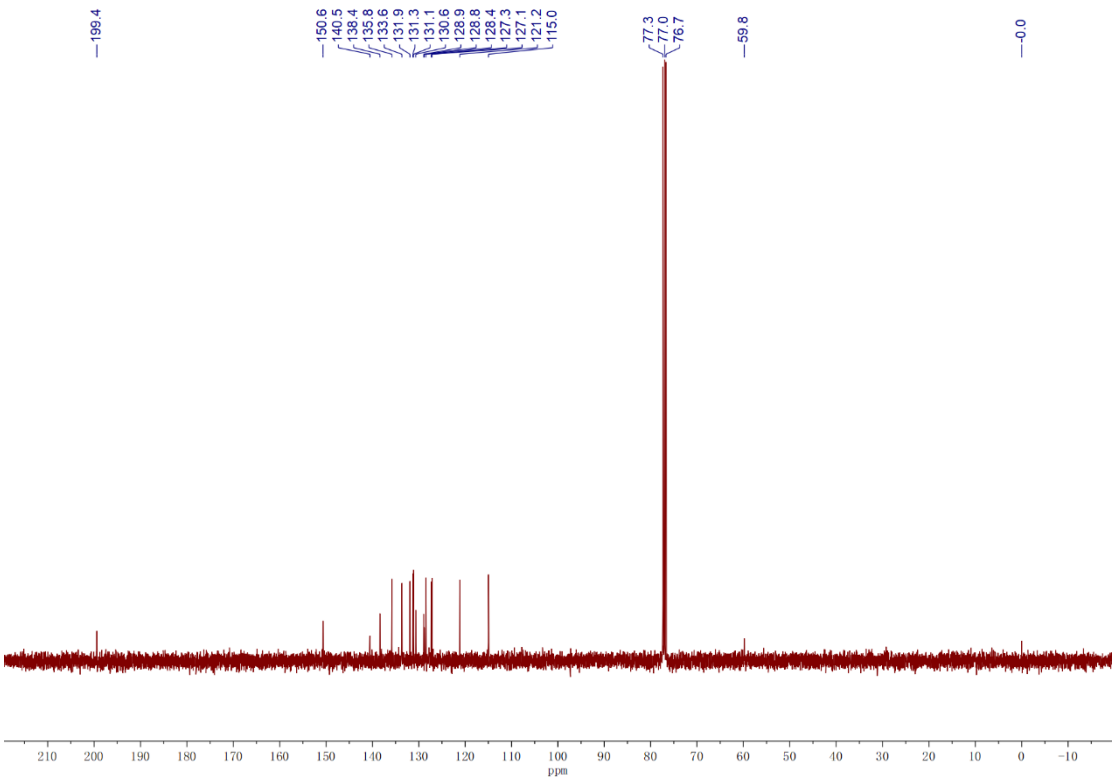

4.15 MALDI-MS (HRMS) plot of 8

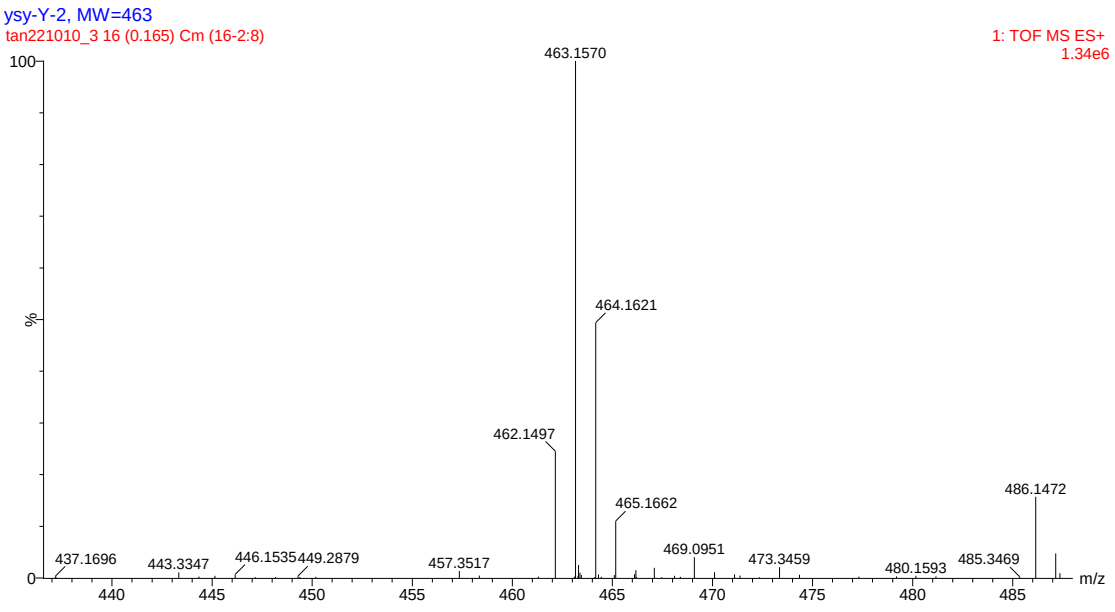

4.16 ^{1}H NMR plot of 9, 400 MHz, $CDCl_3$

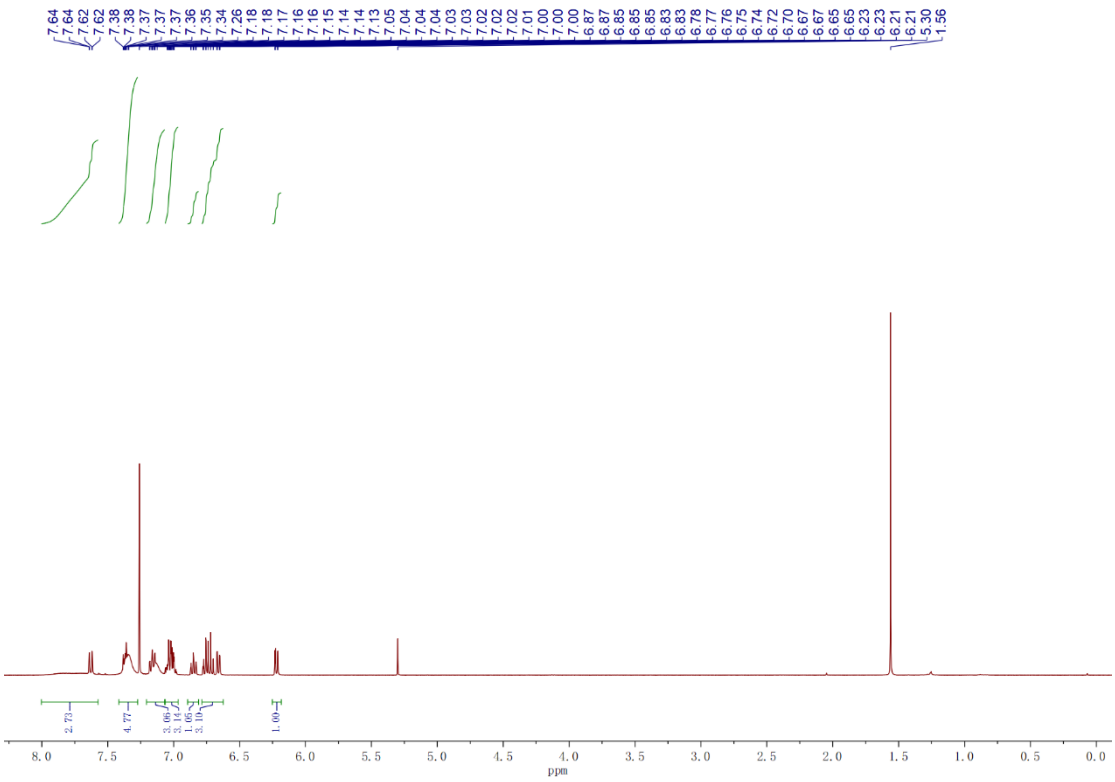

4.17 ^{13}C NMR plot of 9, 101 MHz, $CDCl_3$

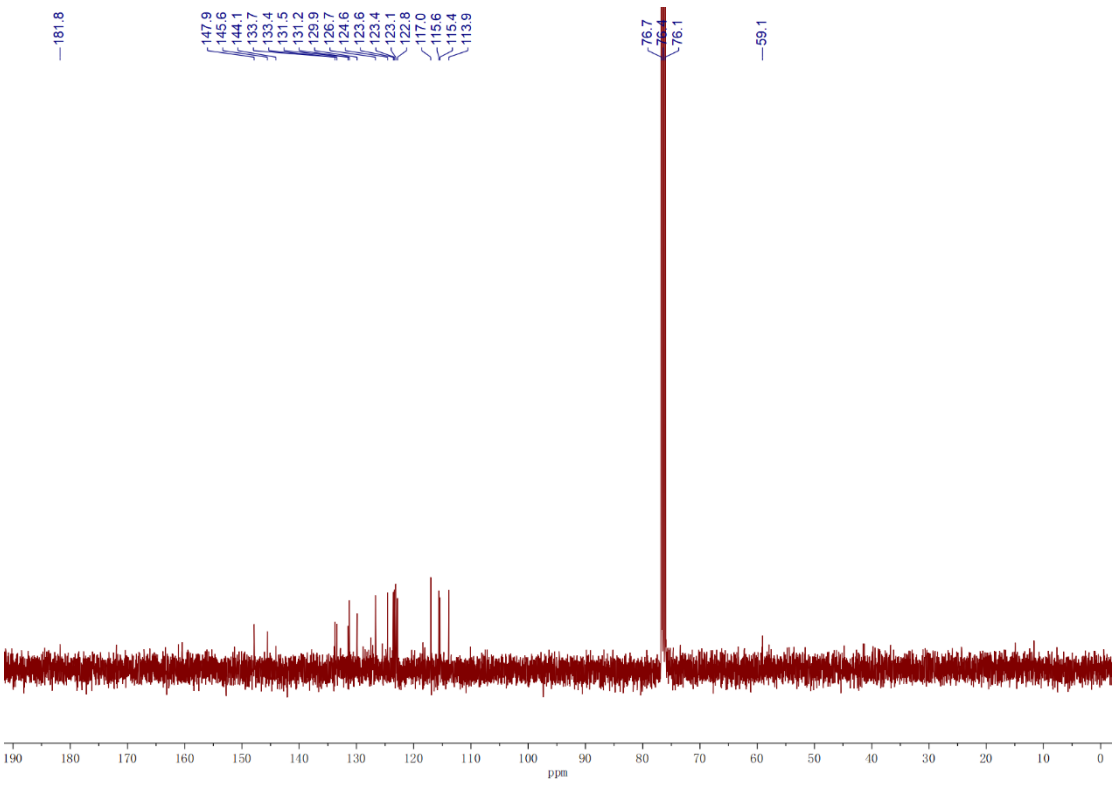

4.18 MALDI-MS (HRMS) plot of 9

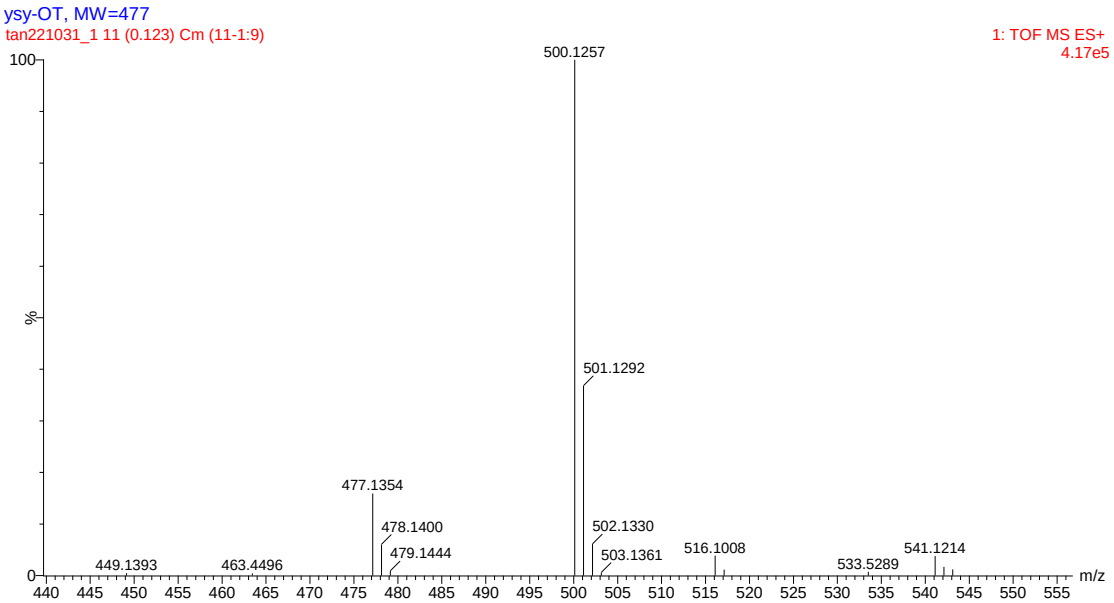

4.19 ^{1}H NMR plot of PCz-Sp-2CN, 400 MHz, $CDCl_3$

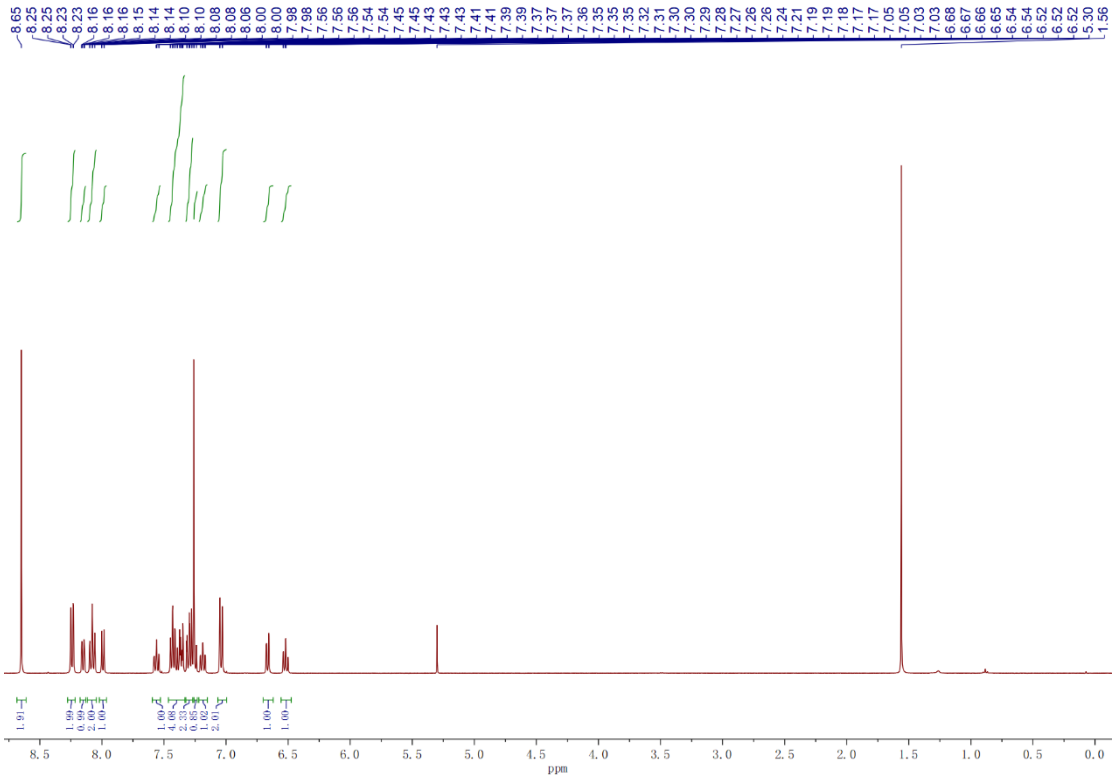

4.20 ^{13}C NMR plot of PCz-Sp-2CN, 101 MHz, $CDCl_3$

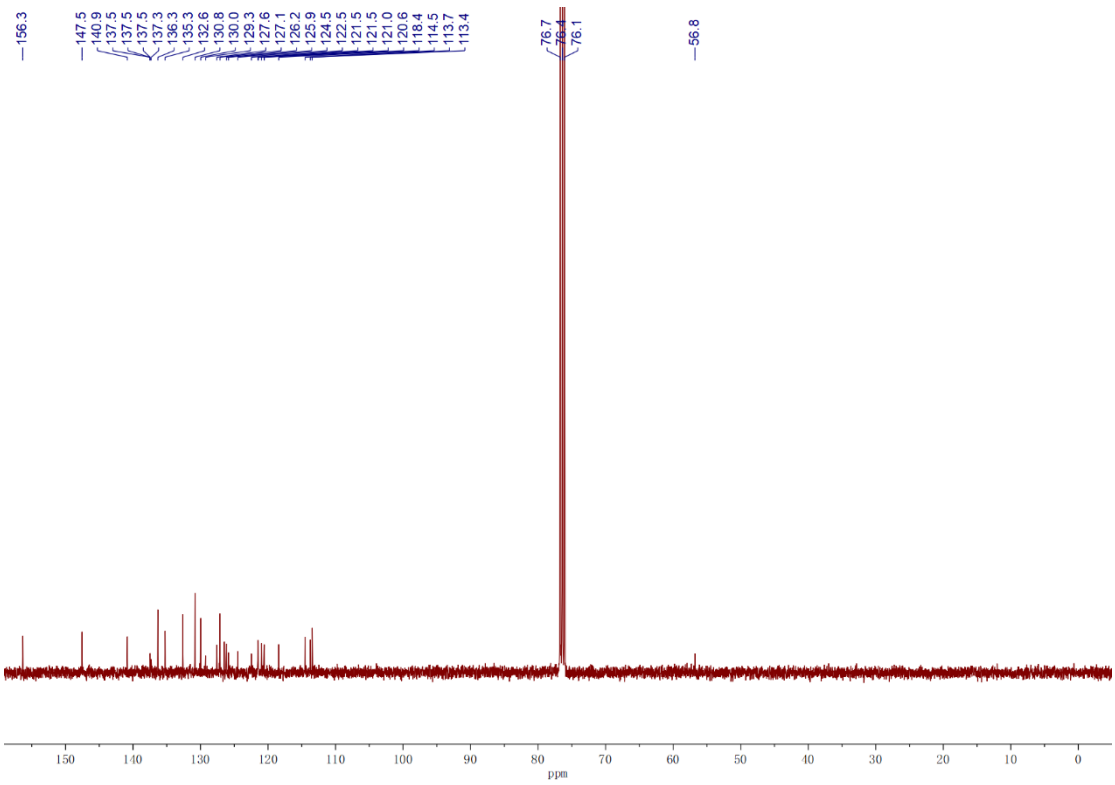

4.21 MALDI-MS (HRMS) plot of PCz-Sp-2CN

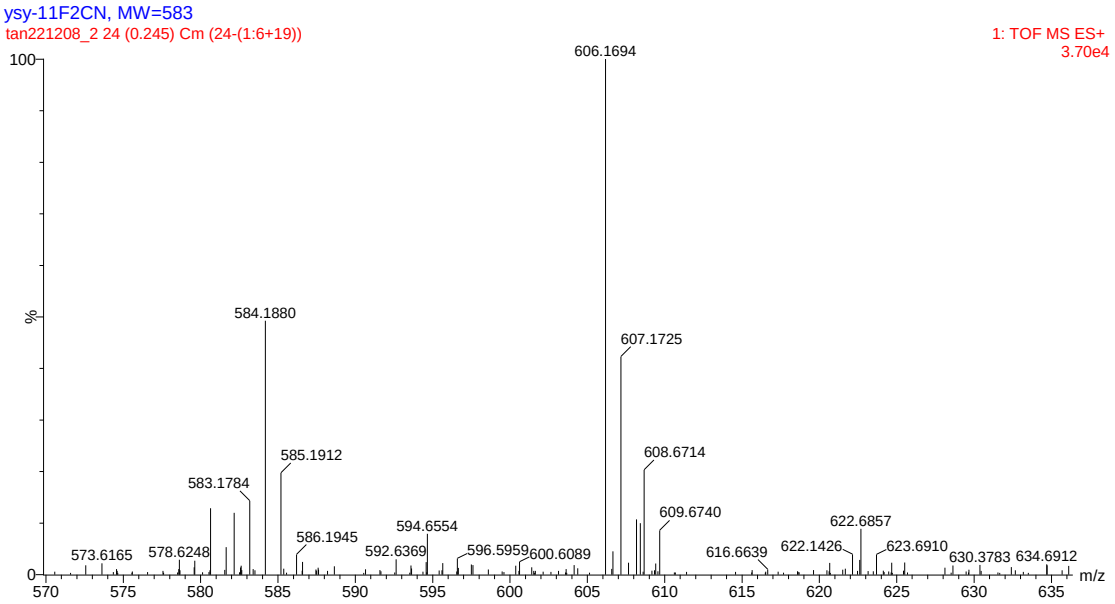

4.22 ^{1}H NMR plot of TPA-Sp-2CN, 400 MHz, $CDCl_3$

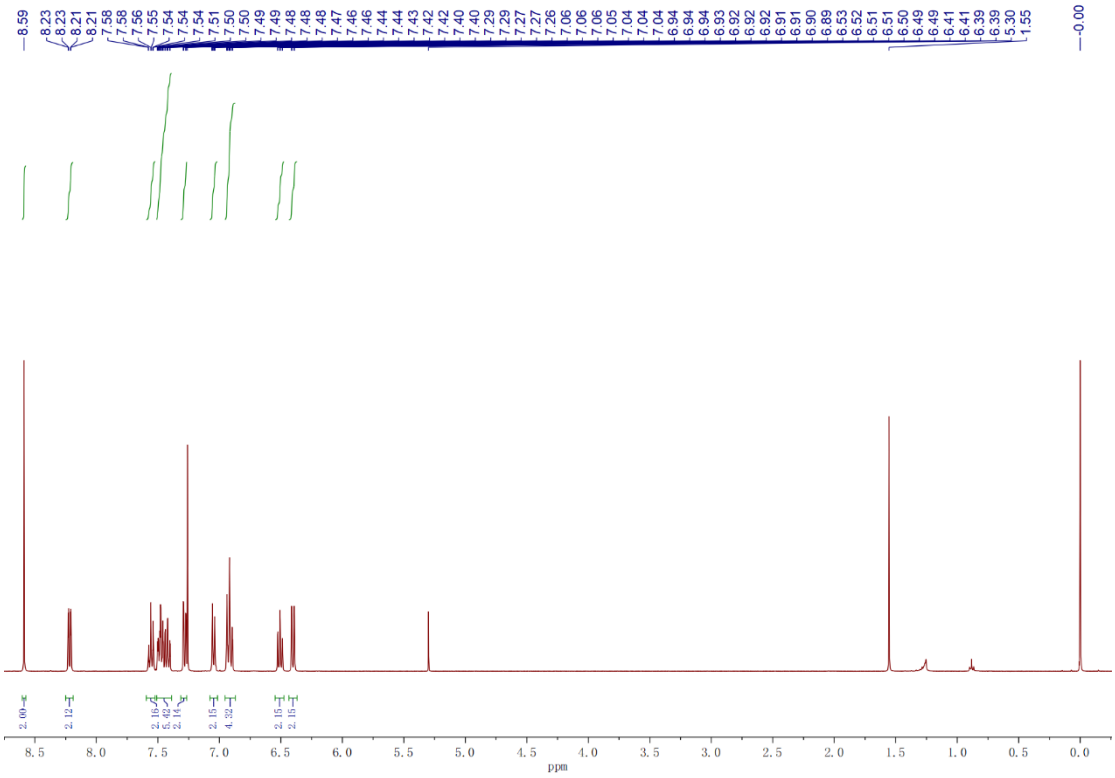

4.23 ^{13}C NMR plot of TPA-Sp-2CN, 101 MHz, $CDCl_3$

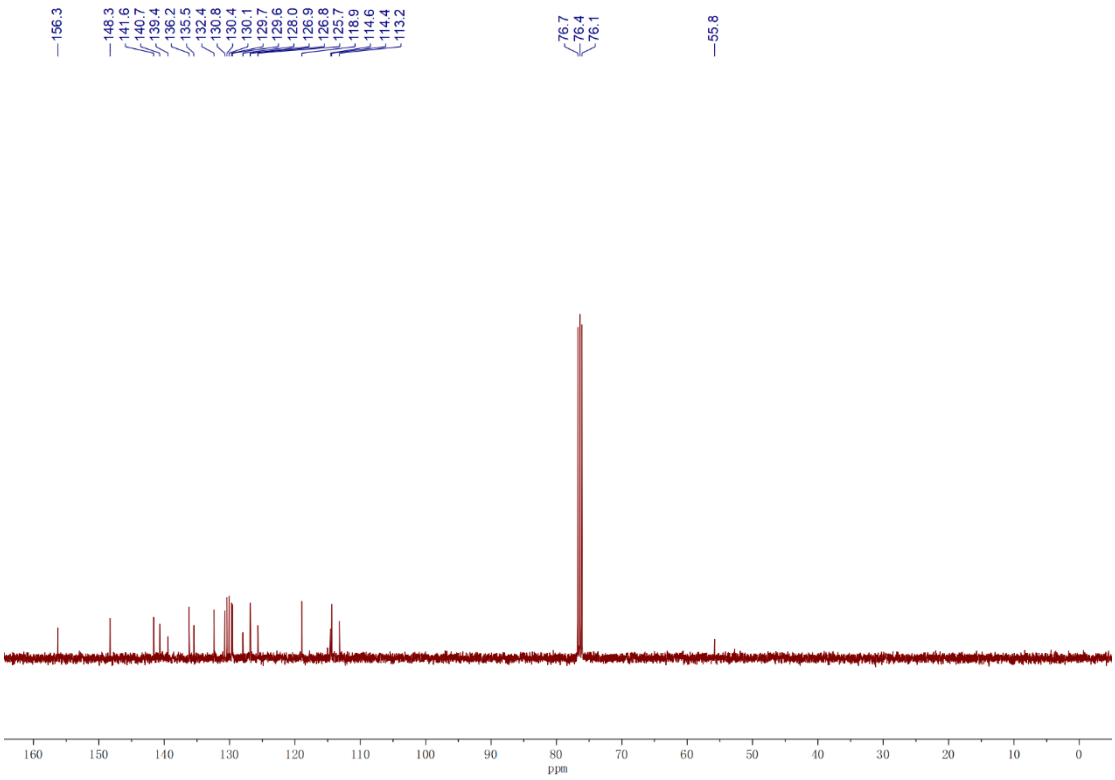

4.24 MALDI-MS (HRMS) plot of TPA-Sp-2CN

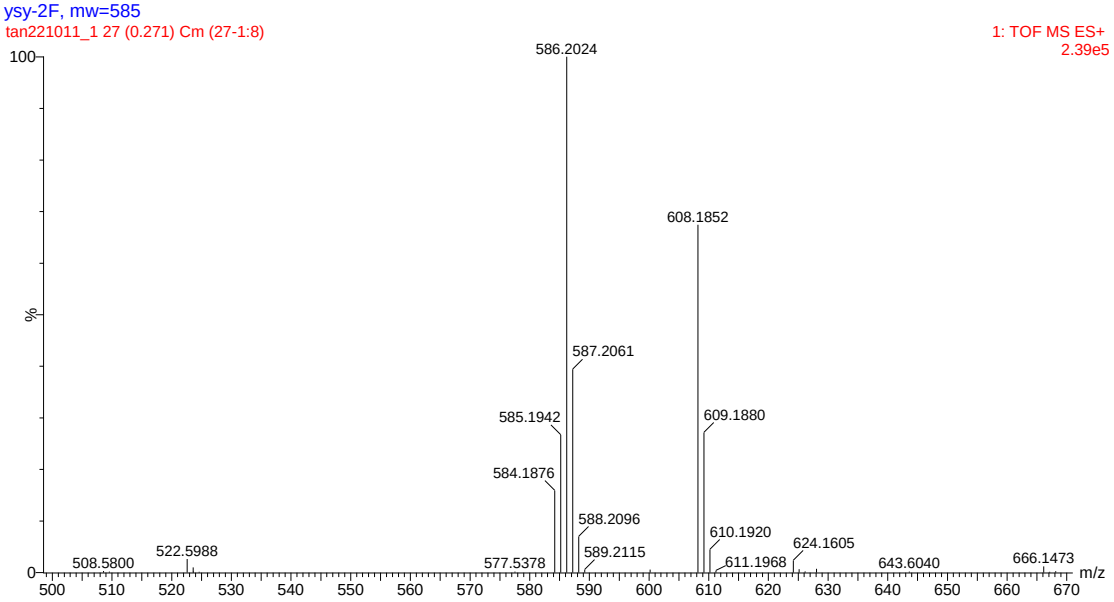

4.25 ^{1}H NMR plot of PXZ-Sp-2CN, 400 MHz, $CDCl_3$

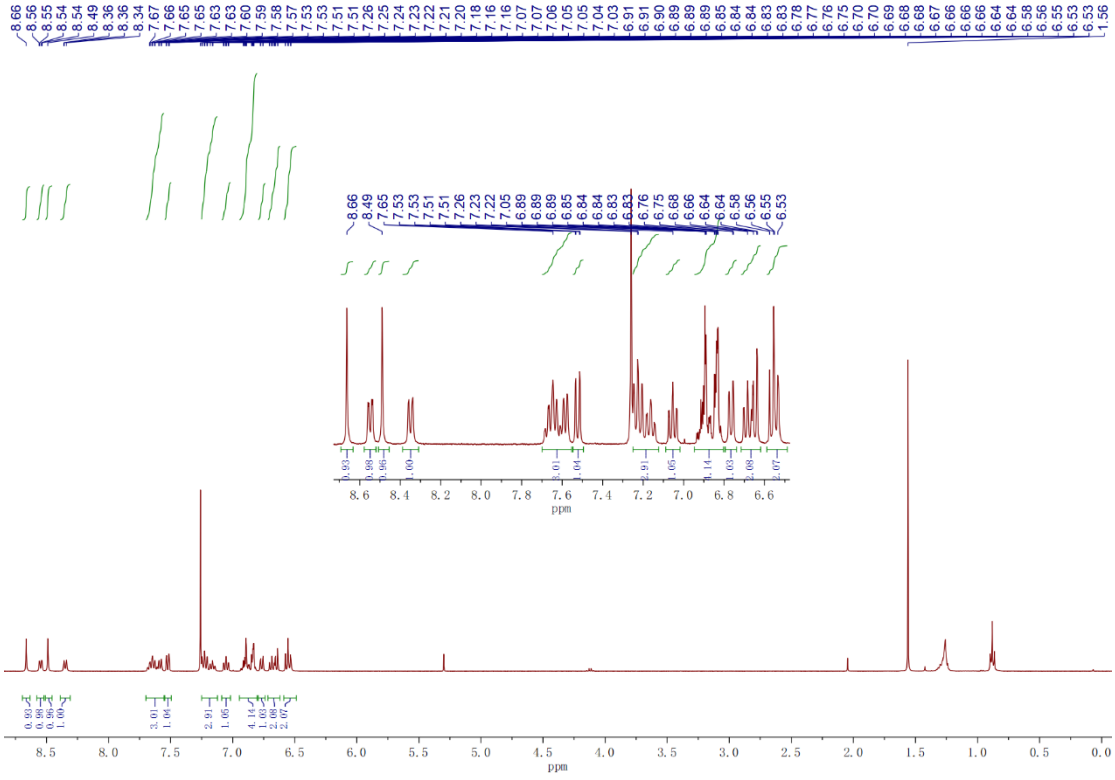

4.26 ^{13}C NMR plot of PXZ-Sp-2CN, 101 MHz, $CDCl_3$

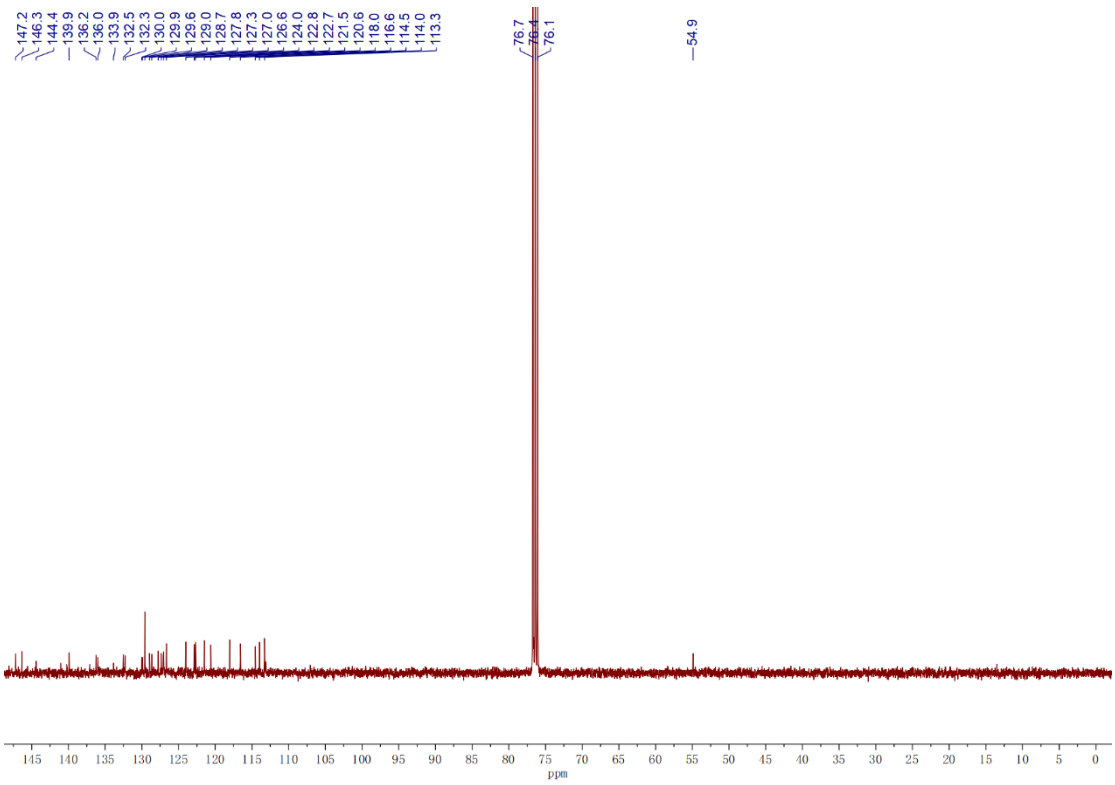

4.27 MALDI-MS (HRMS) plot of PXZ-Sp-2CN

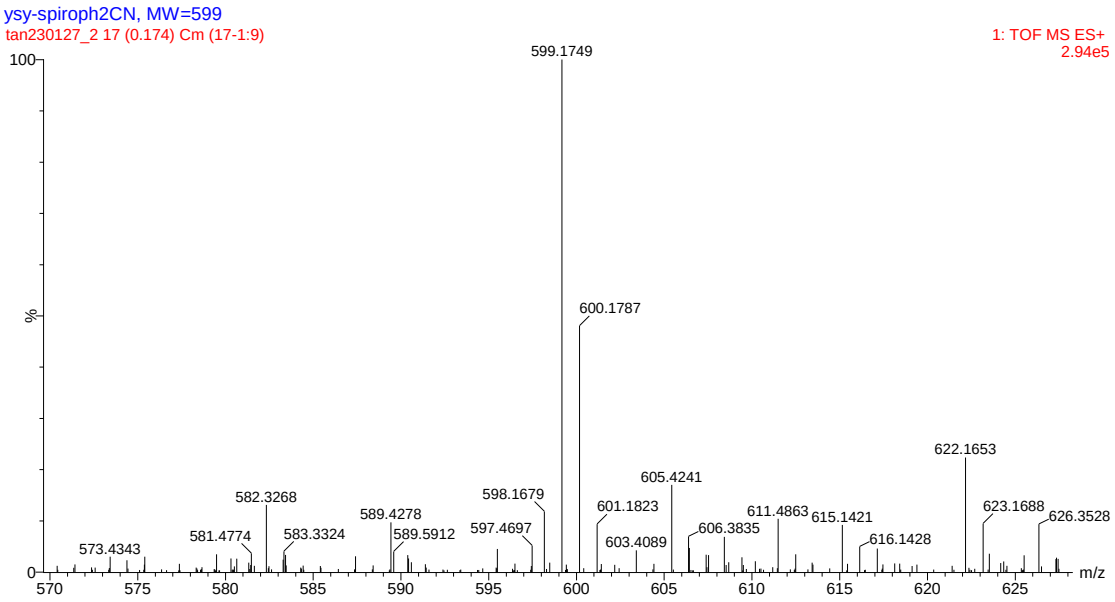

4.28 ^{1}H NMR plot of 2CN, 400 MHz, $CDCl_3$

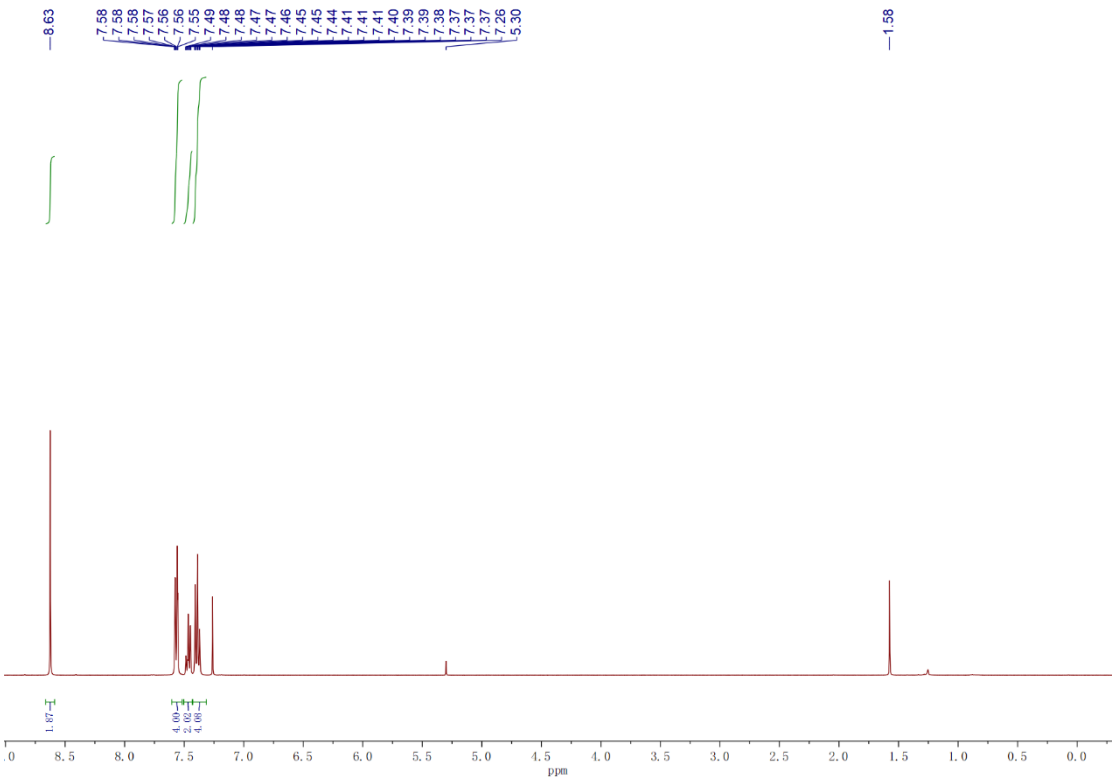

4.29 ^{13}C NMR plot of 2CN, 101 MHz, $CDCl_3$

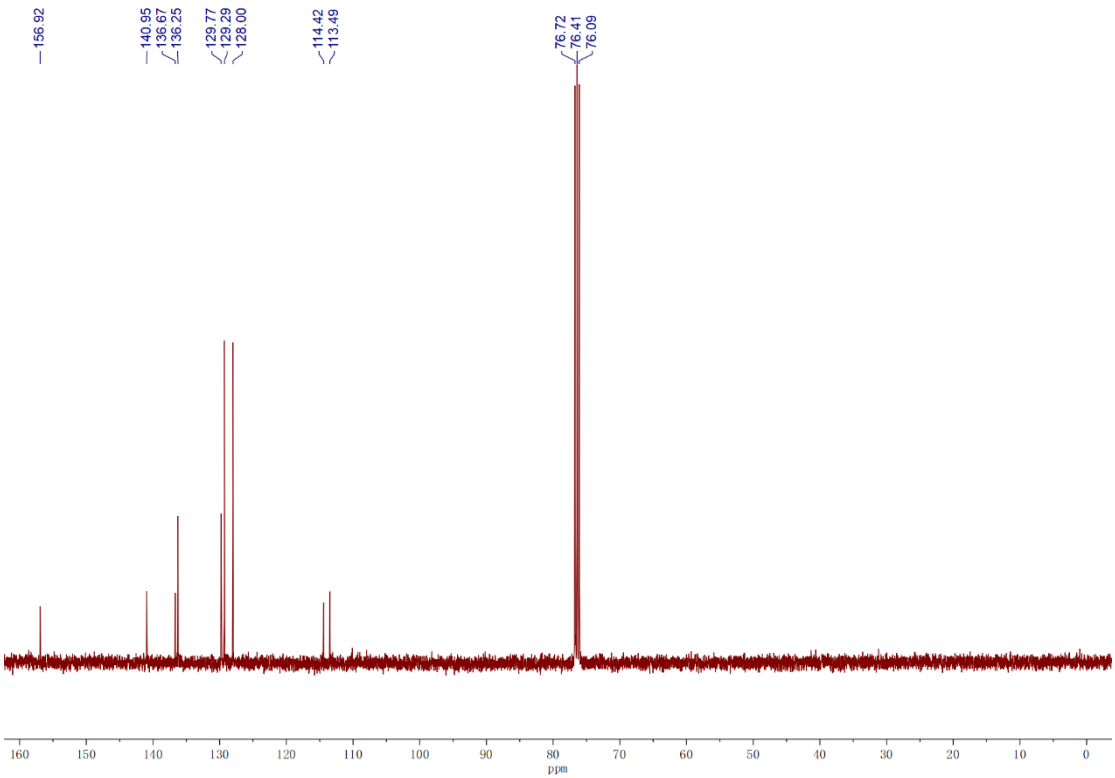

4.30 MALDI-MS (HRMS) plot of 2CN

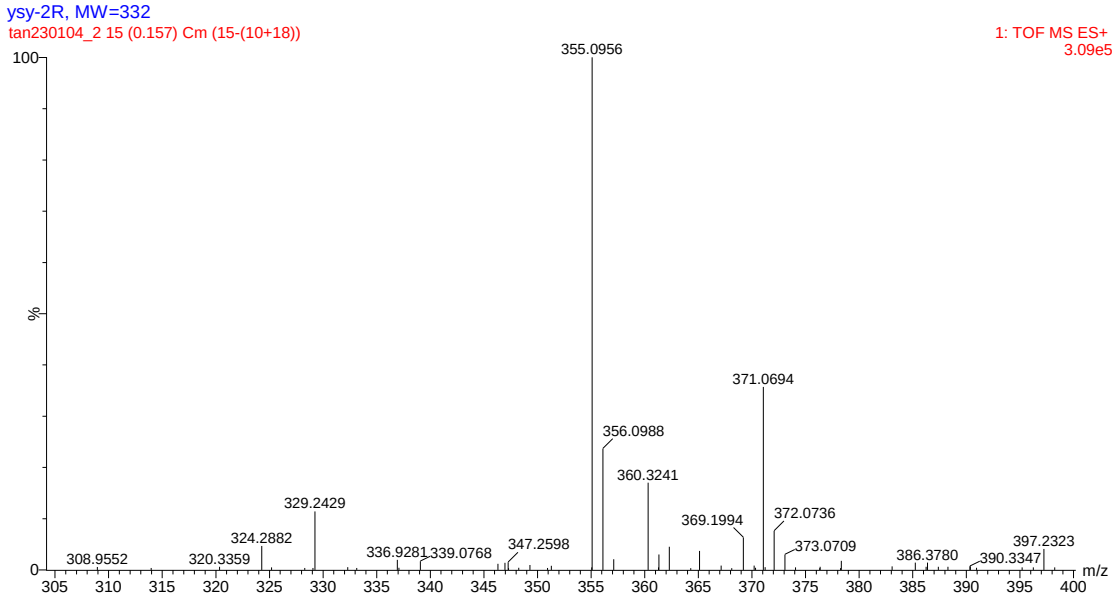

5 References

[1] M. J. Frisch, G. W. Trucks, H. B. Schlegel, G. E. Scuseria, M. A. Robb, J. R. Cheeseman, G. Scalmani, V. Barone, B. Mennucci, G. A. Petersson, H. Nakatsuji, M. Caricato, X. Li, H. P. Hratchian, A. F. Izmaylov, J. Bloino, G. Zheng, J. L. Sonnenberg, M. Hada, M. Ehara, K. Toyota, R. Fukuda, J. Hasegawa, M. Ishida, T. Nakajima, Y. Honda, O. Kitao, H. Nakai, T. Vreven, J. A. Montgomery, Jr., J. E. Peralta, F. Ogliaro, M. Bearpark, J. J. Heyd, E. Brothers, K. N. Kudin, V. N. Staroverov, T. Keith, R. Kobayashi, J. Normand, K. Raghavachari, A. Rendell, J. C. Burant, S. S. Iyengar, J. Tomasi, M. Cossi, N. Rega, J. M. Millam, M. Klene, J. E. Knox, J. B. Cross, V. Bakken, C. Adamo, J. Jaramillo, R. Gomperts, R. E. Stratmann, O. Yazyev, A. J. Austin, R. Cammi, C. Pomelli, J. W. Ochterski, R. L. Martin, K. Morokuma, V. G. Zakrzewski, G. A. Voth, P. Salvador, J. J. Dannenberg, S. Dapprich, A. D. Daniels, O. Farkas, J. B. Foresman, J. V. Ortiz, J. Cioslowski and D. J. Fox, Gaussian, Inc., Wallingford CT, 2013, Gaussian 09, Revision E.01.

[2] Becke, A. D. *J. Chem. Phys.* **1993**, *98*, 5648-5652.

[3] Lee, C.; Yang, W.; Parr, R. G. *Phys. Rev. B*, **1988**, *37*, 785-789.

[4] Lu, T.; Chen, F. *J. Comput. Chem.*, **2012**, *33*, 580-592.

[5] (a) Johnson, E. R.; Keinan, S.; Sanchez, P. M.; Garcıa, J. C.; Cohen, A. J.; Yang, W. *J. Am. Chem. Soc.* **2010**, *132*, 6498–6506; (b) Lefebvre, C.; Rubez, G.; Khartabil, H.; Boisson, J. C.; Garcia, J. C.; Henon, E. *Phys. Chem. Chem. Phys.*, **2017**, *19*, 17928-17936.

[6] Humphrey, W.; Dalke, A.; Schulten, K. *J. Mole. Graph.*, **1996**, *14*, 33-38.

[7] H. Ren, Y. Song, R. Yu, M. Tian, L. He, *Dyes Pigm.* **2022**, *204*, 110389.

[8] J. Liu, Z. Feng, C. Peng, Y. Yu, S. Yang, Z. Jiang, L. Liao, *Chin. Chem. Lett.* **2023**, *34*, 107634.

[9] Z. Zhao, C. Zeng, X. Peng, Y. Liu, H. Zhao, L. Hua, S.-J. Su, S. Yan, Z. Ren, *Angew. Chem. Int. Ed.* **2022**, *61*, e202210864.
[10] Y. Song, M. Tian, R. Yu, L. He, *ACS Appl. Mater. Interfaces* **2021**, *13*, 60269-60278.
[11] Y. Song, Y. Li, R. Yu, K. Zhang, L. He, *Adv. Opt. Mater.* **2023**, *11*, 2300432.
[12] F.-M. Xie, H.-Z. Li, K. Zhang, Y. Shen, X. Zhao, Y.-Q. Li, J.-X. Tang, *Angew. Chem. Int. Ed.* **2022**, *61*, e202213823.
[13] X.-Q. Wang, S.-Y. Yang, Q.-S. Tian, C. Zhong, Y.-K. Qu, Y.-J. Yu, Z.-Q. Jiang, L.-S. Liao, *Angew. Chem. Int. Ed.* **2021**, *60*, 5213-5219.
[14] Q. Zheng, X.-Q. Wang, Y.-K. Qu, G. Xie, L.-S. Liao, Z.-Q. Jiang, *npj Flex. Electron.* **2022**, *6*, 83.
[15] Z. Wang, D. Li, W. Li, J. Zhang, M. Luo, S. Du, X. Zhang, S. Xu, Z. Ge, *Adv. Opt. Mater.* **2023**, *11*, 2300017.
[16] C.-C. Peng, S.-Y. Yang, H.-C. Li, G.-H. Xie, L.-S. Cui, S.-N. Zou, C. Poriel, Z.-Q. Jiang, L.-S. Liao, *Adv. Mater.* **2020**, *32*, 2003885.
[17] H.-C. Li, X. Tang, S.-Y. Yang, Y.-K. Qu, Z.-Q. Jiang, L.-S. Liao, *Chin. Chem. Lett.* **2021**, *32*, 1245-1248.
[18] S.-Y. Yang, Q.-S. Tian, Y.-J. Yu, S.-N. Zou, H.-C. Li, A. Khan, Q.-H. Wu, Z.-Q. Jiang, L.-S. Liao, *J. Org. Chem.* **2020**, *85*, 10628-10637.
[19] X. Tang, L.-S. Cui, H.-C. Li, A. J. Gillett, F. Auras, Y.-K. Qu, C. Zhong, S. T. E. Jones, Z.-Q. Jiang, R. H. Friend, L.-S. Liao, *Nat. Mater.* **2020**, *19*, 1332-1338.
[20] S.-Y. Yang, Y.-K. Wang, C.-C. Peng, Z.-G. Wu, S. Yuan, Y.-J. Yu, H. Li, T.-T. Wang, H.-C. Li, Y.-X. Zheng, Z.-Q. Jiang, L.-S. Liao, *J. Am. Chem. Soc.* **2020**, *142*, 17756-17765.
[21] S.-Y. Yang, Z.-Q. Feng, Z. Fu, K. Zhang, S. Chen, Y.-J. Yu, B. Zou, K. Wang, L.-S. Liao, Z.-Q. Jiang, *Angew. Chem. Int. Ed.* **2022**, *61*, e202206861.
[22] H.-Z. Li, F.-M. Xie, K. Zhang, Y. Shen, W. Zhou, Y.-Q. Li, W.-J. Wang, J.-X. Tang, *Chem. Eng. J.* **2022**, *436*, 135234.
[23] T. Huang, Q. Wang, G. Meng, L. Duan, D. Zhang, *Angew. Chem. Int. Ed.* **2022**, *61*, e202200059.
[24] Z.-Q. Feng, S.-Y. Yang, F.-C. Kong, Y.-K. Qu, X.-Y. Meng, Y.-J. Yu, D.-Y. Zhou, Z.-Q. Jiang, L.-S. Liao, *Adv. Funct. Mater.* **2023**, *33*, 2209708.
[25] R. Pei, J. Lou, G. Li, H. Liu, X. Yin, C. Zhou, Z. Wang, C. Yang, *Chem. Eng. J.* **2022**, *437*, 135222.
[26] Y.-K. Wang, C.-C. Huang, H. Ye, C. Zhong, A. Khan, S.-Y. Yang, M.-K. Fung, Z.-Q. Jiang, C. Adachi, L.-S. Liao, *Adv. Opt. Mater.* **2020**, *8*, 1901150.
[27] Y.-P. Zhang, X. Liang, X.-F. Luo, S.-Q. Song, S. Li, Y. Wang, Z.-P. Mao, W.-Y. Xu, Y.-X. Zheng, J.-L. Zuo, Y. Pan, *Angew. Chem. Int. Ed.* **2021**, *60*, 8435-8440.
[28] X.-D. Zhu, C.-C. Peng, F.-C. Kong, S.-Y. Yang, H.-C. Li, S. Kumar, T.-T. Wang, Z.-Q. Jiang, L.-S. Liao, *J. Mater. Chem. C* **2020**, *8*, 8579-8584.
[29] Y.-P. Zhang, S.-Q. Song, M.-X. Mao, C.-H. Li, Y.-X. Zheng, J.-L. Zuo, *Sci. China Chem.* **2022**, *65*, 1347-1355.
[30] Y.-J. Yu, M. Song, X.-Y. Meng, Y.-K. Qu, X.-Q. Wang, L. Chen, S.-Y. Yang, D.-Y. Zhou, Z.-Q. Jiang, L.-S. Liao, *Org. Lett.* **2023**, *25*, 6024-6028.
[31] Y. Li, Y. Song, K. Zhang, Y. Xiu, P. Wang, M. Tian, L. He, *Dyes Pigm.* **2023**, *219*, 111572.